U.S. DEPARTMENT OF THE INTERIOR
U.S. GEOLOGICAL SURVEY

INTERPRETATION OF AEROMAGNETIC MAP AND RELATED GEOPHYSICAL DATA FOR MOUNT HAYES 1° X 3° QUADRANGLE, ALASKA

by

David L. Campbell[1] and Warren J. Nokleberg[2]

Open-File Report 97-280

Denver, Colorado
1997

[1]USGS Mineral Resource Surveys Program, Central Region, MS 964
Denver Federal Center, Denver CO 80225-0046
[2]USGS Mineral Resource Surveys Program, Western Region, MS 904,
345 Middlefield Road, Menlo Park CA 94025

INTERPRETATION OF AEROMAGNETIC MAP AND RELATED GEOPHYSICAL DATA FOR MOUNT HAYES 1° x 3° QUADRANGLE, ALASKA

by David L. Campbell and Warren J. Nokleberg

LIST OF FIGURES AND TABLES

INTRODUCTION

This report presents a geologic interpretation of the aeromagnetic map and related geophysical data for the Mount Hayes 1° x 3° quadrangle, eastern Alaska Range, Alaska, (Plate 1), discusses prominent aeromagnetic features and their possible geologic sources, and models three profiles to indicate possible magnetic sources along the profiles. Although this report focuses mainly on aeromagnetic data, the interpretations also make some use of gravity and radiometric maps and of geoelectric soundings. Approximate locations of some magnetic source bodies and of strong magnetic lineaments that may reflect faults are shown on Plate 2. An approximate classification of the source bodies is also made on Plate 2, indicating whether the source bodies are thought to be shallow or intermediate in depth and whether their susceptibility is thought to be high or medium. For most of these bodies, however, no precise analysis of these parameters was done, so that the classification must be regarded as generalized.

GEOLOGY

The Mount Hayes quadrangle is in the eastern Alaska Range, a great glacially-sculpted arcuate mountain range that forms a major geographic boundary between the Yukon River basin of interior Alaska to the north, and the Copper River basin of southern Alaska to the south (fig. 1). The eastern Alaska Range is characterized by high peaks ranging to over 4,180 m in elevation and spectacular valley glaciers up to 65 km long. The range is bisected by the Denali fault, a major tectonic element of south-central Alaska. North of the Denali fault, the bedrock geology is dominated by the Devonian and Mississippian or older Yukon-Tanana terrane, a complex of multiple deformed and metamorphosed sedimentary, igneous, and plutonic rocks (Jones and others, 1981; Nokleberg and Aleinikoff, 1985). To the south the bedrock geology is dominated by the Mesozoic Maclaren, and the

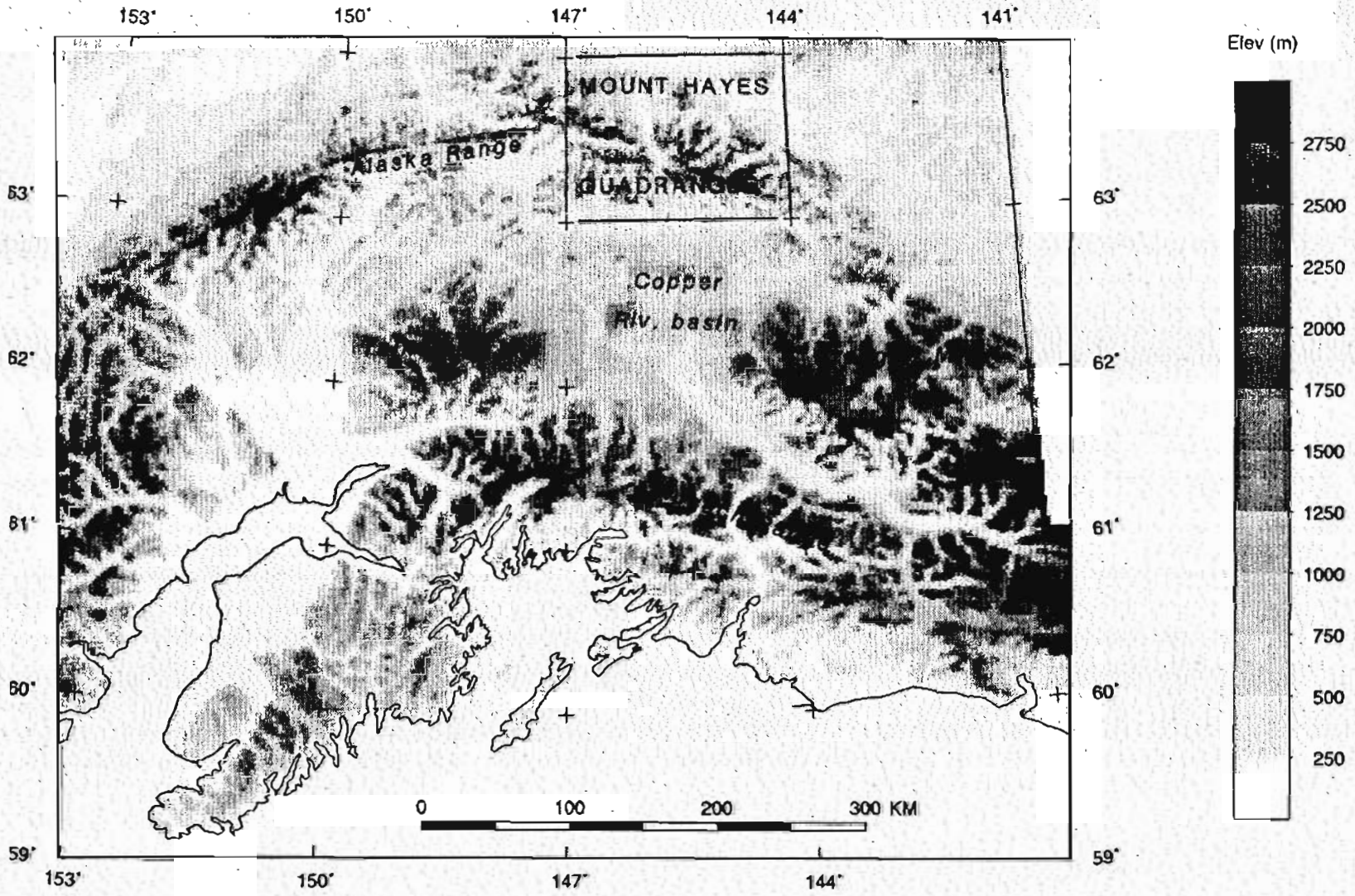

Figure 1.--Topographic map of south-central Alaska, showing regional setting of the Mount Hayes quadrangle.

Paleozoic and Mesozoic Wrangellia terranes (Jones and others, 1981; Nokleberg and others, 1982, 1985). A moderate number of granitic and lesser gabbroic plutons, chiefly of Mesozoic age, occur both north and south of the Denali fault, as well as major faults and sutures separating terranes, and younger Cenozoic faults that occur chiefly within terranes.

Bedrock geology maps of parts of the Mount Hayes quadrangle have been published by Rose (1965; 1966a,b; 1967), Rose and Saunders (1967); Matteson (1973), Bond (1976), Stout (1976) Richter and others (1977), Nokleberg and others (1982), and Nokleberg, Aleinikoff, Lange and others (1992). The geologic base for Plate 2 is based partly on that geology and to a greater degree on 1:63,360 scale geologic mapping of the entire quadrangle that was done for the Alaska Mineral Resource Assessment Program (AMRAP). This report is part of a folio of reports on the Mount Hayes quadrangle prepared under AMRAP by U.S. Geological Survey personnel. Companion reports in the folio include geologic maps by Nokleberg, Aleinikoff, Lange and others (1992), geochemical studies by Curtin and others (1989), a compilation of isotopic and fossil age data by Nokleberg, Aleinikoff, Dutro and others (1992), a compilation of mineral deposits by Nokleberg and others (1991), and a study of the mineral resource potential of the quadrangle by Nokleberg and others (1990). A recent overview of the geology of south-central Alaska, describing the regional geologic setting of the Mount Hayes quadrangle, was published by Nokleberg and others (1994).

The Mount Hayes quadrangle contains a series of accreted tectonostratigraphic terranes (Jones and others, 1981; Nokleberg and others, 1982), fault-bounded entities which are structurally and stratigraphically distinct from nearby terranes (fig. 2). South of the Denali fault are the Wrangellia, Maclaren, Clearwater, and Gulkana River terranes, and the terrane of ultramafic and associated rocks. The terranes are juxtaposed along a number of thrust and strike-slip faults which trend subparallel to the Denali Fault. These thrusts include the Broxson Gulch thrust, which forms the boundary between the Wrangellia and Maclaren terranes; the Eureka Creek thrust, which separates two subterranes of Wrangellia, the Slana River subterrane on the north and the Tangle subterrane on the south; and the Paxson Lake fault, which forms the boundary between the Tangle subterrane to the north and the Gulkana River terrane to the south. North of the Denali Fault are the Aurora Peak, Windy and Yukon-Tanana terranes. Four subterranes of the Yukon-Tanana terrane, the Hayes Glacier subterrane, the Jarvis Creek Glacier subterrane, the Macomb subterrane and the Lake George subterrane, have been recognized in the Mount Hayes quadrangle (Nokleberg and Aleinikoff, 1985). The faults dividing these terranes include the Nenana Glacier fault, separating the Aurora Peak terrane from

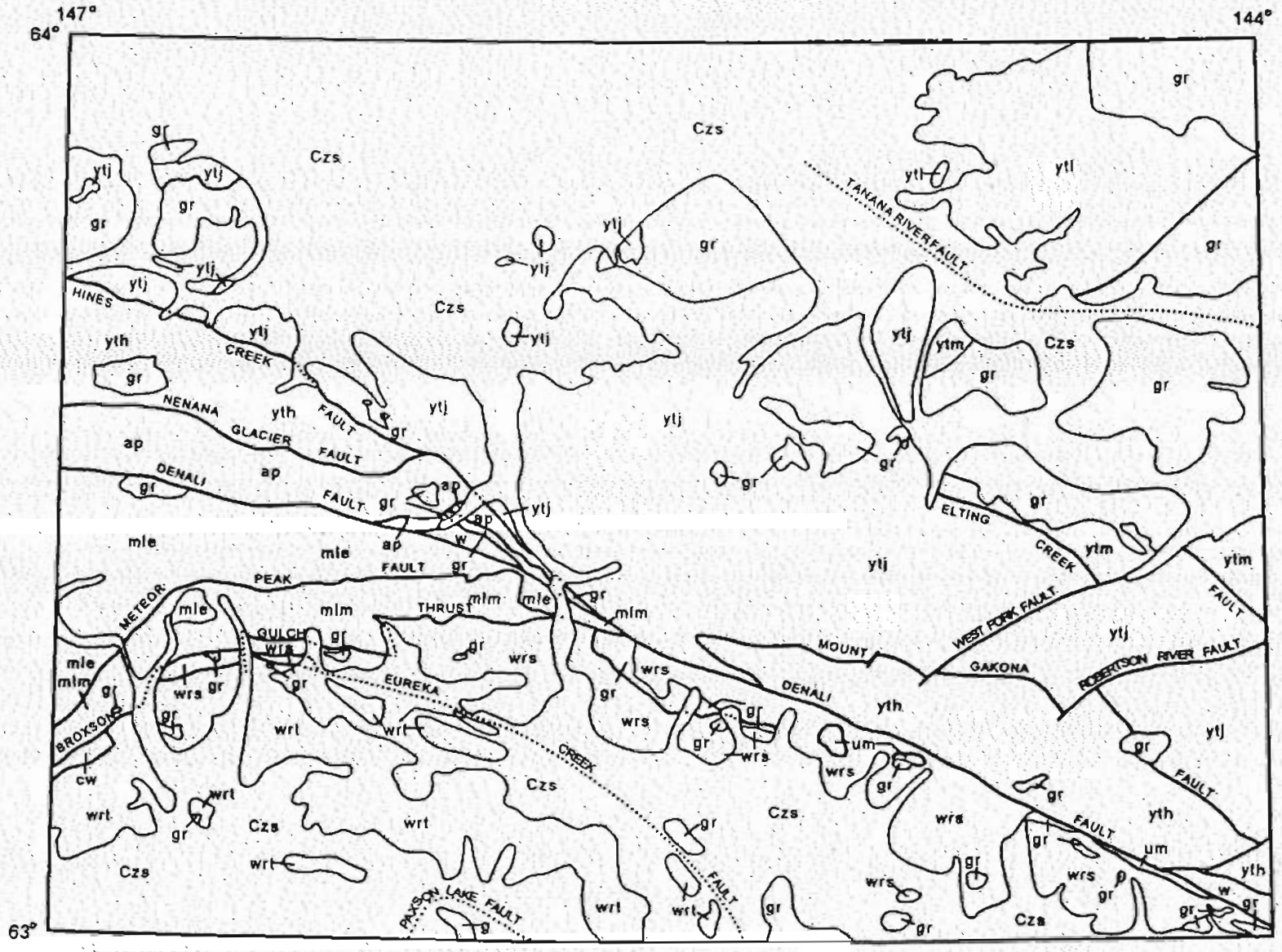

Figure 2.--Tectonostratigraphic terranes and subterranes in the Mount Hayes quadrangle. Scale about 1/500,000.

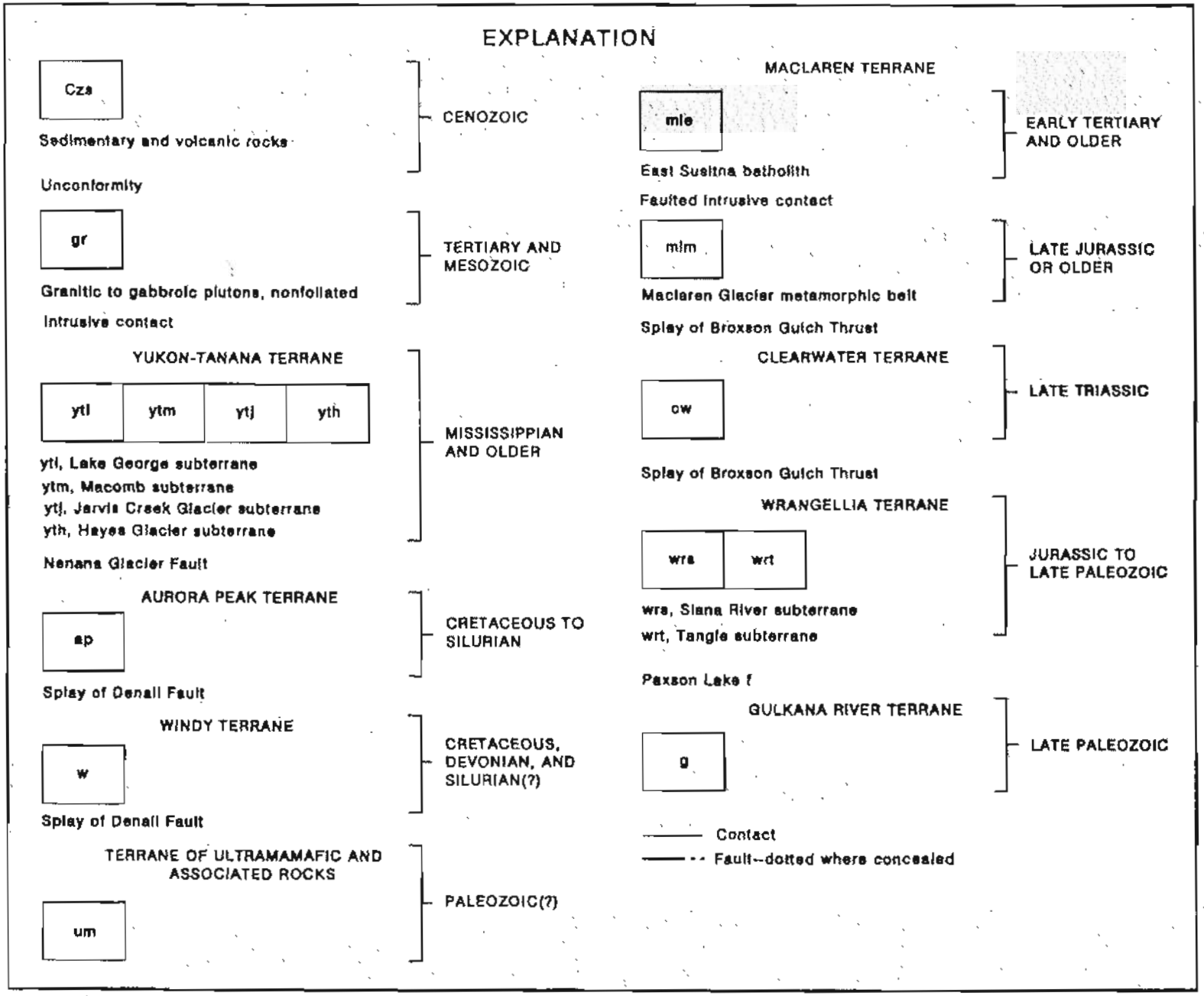
EXPLANATION
Cza
CENOZOIC
Sedimentary and volcanic rocks
Unconformity
gr
TERTIARY AND MESOZOIC
Granitic to gabbroic plutons, nonfoliated
Intrusive contact
YUKON-TANANA TERRANE
ytl
ytm
ytj
yth
MISSISSIPPIAN AND OLDER
ytl, Lake George subterrane
ytm, Macomb subterrane
ytj, Jarvis Creek Glacier subterrane
yth, Hayes Glacier subterrane
Nenana Glacier Fault
AURORA PEAK TERRANE
ap
CRETACEOUS TO SILURIAN
Splay of Denali Fault
WINDY TERRANE
w
CRETACEOUS, DEVONIAN, AND SILURIAN(?)
Splay of Denali Fault
TERRANE OF ULTRAMAMAFIC AND ASSOCIATED ROCKS
um
PALEOZOIC(?)
MACLAREN TERRANE
mle
EARLY TERTIARY AND OLDER
East Susitna batholith
Faulted intrusive contact
mlm
LATE JURASSIC OR OLDER
Maclaren Glacier metamorphic belt
Splay of Broxson Gulch Thrust
CLEARWATER TERRANE
cw
LATE TRIASSIC
Splay of Broxson Gulch Thrust
WRANGELLIA TERRANE
wra
wrt
JURASSIC TO LATE PALEOZOIC
wra, Slana River subterrane
wrt, Tangle subterrane
Paxson Lake f
GULKANA RIVER TERRANE
g
LATE PALEOZOIC
Contact
Fault--dotted where concealed

the Hayes Glacier subterrane of the Yukon Tanana terrane; the Hines Creek fault, separating both from the Jarvis Creek Glacier subterrane of the Yukon-Tanana terrane; and the Mount Gakona fault, separating the eastern part of the Hayes Glacier subterrane from the Jarvis Creek Glacier subterrane. The Elting Creek fault separates the Jarvis Creek Glacier and Macomb subterranes, and the Tanana River fault separates the Macomb and Lake George subterranes.

Terranes South of Denali Fault

The Wrangellia terrane (Jones and others, 1981) is predominantly composed of Paleozoic island arc rocks which are disconformably overlain by the Triassic Nikolai Greenstone and locally by younger rocks. Nokleberg and others (1981a) have recognized two subterranes of Wrangellia. The Slana River subterrane, to the north, consists of andesite flows, breccia, epiclastic rocks, argillite, and limestone of Pennsylvanian to Permian age (Richter and others, 1977). The Triassic Nikolai Greenstone, which disconformably overlies this island arc sequence, consists of massive, subaerial, amydgaloidal basalt flows. Compared with the Slana River subterrane, the Tangle subterrane to the south contains a much thinner sequence of upper Paleozoic rocks, but a much thicker sequence of overlying Nikolai Greenstone rocks. The upper Paleozoic rocks of the Tangle subterrane are predominantly aquagene tuff with minor andesite. Extensive gabbro dikes, sills, and stratiform cumulate mafic and ultramafic rock intrude the sedimentary and volcanic rock of the Tangle subterrane.

South of the Paxson Lake fault are rocks of the metamorphic complex of Gulkana River (Nokleberg and others, 1986), called the Gulkana River terrane by Nokleberg, Aleinikoff, Lange, and others (1992) and called the southern Wrangellia terrane by Plafker and others (1989). The only rocks of this complex that crop out in the Mount Hayes quadrangle are those of a schistose metaandesite unit around longitude 146° W on the extreme southern border of the quadrangle.

The Maclaren terrane (Jones and others, 1981) is composed of penetratively deformed and regionally metamorphosed plutonic rocks, and schist, phyllite, argillite and metagraywacke. The northern part of the Maclaren terrane consists of the East Susitna batholith, predominantly metamorphosed diorite and graodiorite with lesser quartz monzonite. The southern part consists of the Maclaren Glacier metamorphic belt, metasedimentary rocks that increase northward in metamorphic grade from lower greenschist facies to amphibolite facies metamorphism.

The Clearwater terrane (Jones and others, 1981) consists of a small fault-bounded block of highly deformed chlorite schist,

muscovite schist, schistose rhyodacite, marble, and greenstone derived from basalt. The unit exhibits a weakly-developed greenschist facies metamorphism. Many map units exhibit primary bedding and sedimentary or volcanic textures or structures. The Clearwater terrane is intruded by one pluton of weakly-deformed, metamorphosed diorite and quartz diorite.

Terranes North of Denali Fault

The Aurora Peak terrane (Nokleberg and Aleinikoff, 1985) consists predominantly of fine- to medium-grained and poly-deformed calc-schist, marble, quartzite, and pelitic schist, with lesser amounts of regionally metamorphosed and deformed Cretaceous and early Tertiary plutonic rocks. The terrane has been twice cataclastically deformed and twice regionally metamorphosed at upper amphibolite and middle greenschist facies into mylonitic schist and blastomylonite.

The Windy terrane (Jones and others, 1981) consists predominantly of argillite, limestone, and coarser clastic rocks. It is generally weakly deformed, locally exhibiting incipient greenschist facies metamorphism. The Windy terrane exhibits primary bedding, and sedimentary and volcanic textures and structures in appropriate units. It is intruded locally by dikes of metagabbro and diabase.

Yukon-Tanana Terrane

Four subterranes of the Yukon-Tanana terrane occur in the Mount Hayes quadrangle. From south to north, these are the Hayes Glacier subterrane, the Jarvis Creek Glacier subterrane, the Macomb subterrane, and the Lake George subterrane. The Hayes Glacier subterrane of the Yukon-Tanana terrane (Nokleberg and Aleinikoff, 1985) consists predominantly of fine-grained, poly-deformed phyllite that is subdivided into two members: a metasedimentary rock member with little or no metavolcanic rock; and a metavolcanic rock member with moderate amounts of metasedimentary rock. Both members are cataclastically deformed and regionally metamorphosed at lower and middle greenschist facies. The Hayes Glacier subterrane is intruded by intensely deformed and metamorphosed mafic dikes, which crosscut schistosity and foliation in both metasedimentary and metavolcanic rocks.

The Jarvis Creek Glacier subterrane of the Yukon-Tanana terrane (Aleinikoff and Nokleberg, 1985) consists predominantly of fine-grained, poly-deformed schist that is subdivided into two major members: a metasedimentary rock member; and a metavolcanic rock member with moderate amounts of metasedimentary rock. Both members are cataclastically deformed and regionally metamorphosed at greenschist facies into mylonitic schist and local phyllonite.

Large areas of upper greenschist facies and lower amphibolite facies metamorphism occur in the northern part of the subterrane, but the higher-grade minerals retrogressively replaced by lower-grade minerals from north to south. The Jarvis Creek Glacier subterrane is intruded by intensely deformed and metamorphosed mafic dikes (Cretaceous?), and by non-schistose monzonite and alkali gabbro intrusions and lamprophyre dikes (late Cretaceous and early Tertiary). There are many massive sulfide deposits and occurrences in the Jarvis Creek Glacier subterrane (Nokleberg and others, 1990).

The Macomb subterrane of the Yukon-Tanana terrane (Nokleberg and Aleinikoff, 1985) consists predominantly of cataclastically deformed sedimentary and plutonic rocks which have been regionally metamorphosed at epidote- amphibolite facies to upper greenschist facies into mylonitic schist. Subunits are: (1) an older, poly-deformed, medium-grained pelitic schist, calc-schist, and feldspar-quartz-biotite schist derived from shale, marl, and sandstone of Devonian or older age; and (2) a suite of relatively younger, shallow-level, fine- to medium-grained schistose granite, granodiorite, quartz diorite, and diorite of Devonian age. The Macomb subterrane is intruded by less deformed and metamorphosed middle-Cretaceous and possibly younger granitic rocks ranging in composition from quartz diorite to granite.

The Lake George subterrane of the Yukon-Tanana terrane (Nokleberg and Aleinikoff, 1985) consists predominantly of pelitic sedimentary and plutonic rocks that have been cataclastically deformed and regionally metamorphosed at upper amphibolite facies into mylonitic schist and mylonitic gneiss, and which exhibit local retrogression to the lower greenschist facies. Subunits are: (1) a poly-deformed, coarse-grained pelitic muscovite-quartz-biotite-garnet schist derived from quartz-rich to clay-rich shale of Devonian or older age, and (2) relatively younger Devonian and Mississippian medium-grained schistose granodiorite and diorite, and coarse-grained augen gneiss derived from granite and granodiorite. The Lake George subterrane is intruded by middle Cretaceous and possibly early Tertiary diorite, granodiorite, and granite, now weakly metamorphosed under conditions of lower greenschist facies. Small areas of some plutons are extensively hydrothermally altered.

AEROMAGNETIC MAPS

Plate 1 shows an aeromagnetic map of the Mount Hayes quadrangle (State of Alaska, 1974). The survey was flown in 1962-3 by LKB Company under contract to the State of Alaska. It was nominally flown draped 1000 ft (304 m) above mean terrain, with lines oriented north-south and spaced 3/4 mile (1.2 km) apart. The data were compiled at a scale of 1:63,360 and

delivered to the State as analog contour maps.

For safety reasons, the survey aircraft could not maintain the 1000-foot drape contract specification over rugged terrain in the Mount Hayes quadrangle. Analog records showing true ground clearances were supplied to the State with the contour maps, but have since been lost (John Decker, oral commun., March, 1982). Griscom (1977) examined such records for the survey of the nearby Tanacross quadrangle and found the contractor was able to hold specifications only over the ridge crests; the aircraft sometimes flew 500 to 1000 m above valley floors. The most likely effect of departures from true draped conditions is to somewhat smooth the resulting magnetic fields. (See Grauch and Campbell, 1983, for a fuller discussion.)

A regional field of 56,535 gammas (1 gamma = 1 nanoTesla, nT) magnitude at the southwest corner of Plate 1 and increasing approximately 3.2 nT/km, N52E, was removed by the contractor. This regional field equals the International Geomagnetic Reference Field for the year of the survey, and it varies somewhat over the 24 15-minute quadrangles which make up the map. The progression of low-interval contours across the central, low-magnetic, portion of Plate 1 indicates, however, that an additional regional field may still be present. The size and direction of this residual regional field appears to be approximately 4.7 nT/km, N35E, along the eastern border of the map, grading to 1.5 nT/km, due N, along its western border. As will be shown below, this additional regional field is probably a magnetic polarity effect due to sequences of highly magnetic rocks that occur in the Wrangellia terrane.

The aeromagnetic field depicted on Plate 1 reflects the presence of magnetic minerals in nearby rocks, such as magnetite (by far most common) or pyrrhotite (possibly important locally). The magnetizations causing these fields may be "induced", i.e., caused by the Earth's present-day magnetic field; or they may be "remanent", existing more-or-less permanently in the rocks due to processes which took place in the past. Strong remanent magnetizations are found mostly in mafic volcanic rocks, whereas induced magnetizations generally typify plutonic and metamorphic rocks. Most sedimentary rocks are non-magnetic. At high magnetic latitudes, as in Alaska, the highest magnetic field values usually occur over the causative bodies of rocks. All magnetic bodies have regions of low magnetic field values, as well as highs, associated with them, though the lows are sometimes too diffuse to be seen, or are obscured by fields from other bodies. For bodies with induced magnetizations, the low will occur to the magnetic north of the body (in the northern hemisphere), but for bodies with strong remanence it may occur in some other direction.

The original analog data on Plate 1 has recently been

digitized and merged with other aeromagnetic surveys to make a uniform digital aeromagnetic map of south-central Alaska (Meyer and Saltus, 1995). That regional map was compiled by Patterson, Grant, and Watson, Ltd., of Toronto, Ontario, under a contract to the State of Alaska Department of Natural Resources. The Mount Hayes part of the data did not undergo any further re-leveling, nor were any data trends removed from it, during compilation (Patterson, Grant, and Watson, Ltd., unpublished report, April 19, 1995). Fig. 3 shows two color-shaded-relief (CSR) maps of these compiled digital data. This CSR representation treats the aeromagnetic field data as a topographic surface, which will cast shadows when illuminated by a computer-driven "sun". The sun azimuth and angle of elevation can be adjusted to bring out features of interest in the data. For Fig. 3 the sun azimuth is 220° and sun elevation is 60°, values chosen to emphasize features trending parallel to the Denali Fault. Fig. 3a shows observed aeromagnetic fields as compiled by Patterson, Grant, and Watson (Meyer and Saltus, 1995). On this map sharp magnetic gradients will occur along the north edges of bodies of rocks that have high magnetic susceptibilities ("source bodies"). Fig. 3b shows reduced-to-pole magnetic data; data, that is, which have been processed mathematically to simulate fields that would be seen at a place where the Earth's magnetizing field is vertically down (the north magnetic pole). Such processing subdues polarity lows and shifts magnetic highs so that they fall directly over source bodies, but it leaves low magnetic "skirts" that extend beyond the edges of the source bodies on all sides. The above generalizations suppose that the source rocks are all magnetized along the direction of the Earth's magnetic field; they can be wrong if the source rocks have strong remanent magnetizations in other directions.

An important difference between figs. 3a and 3b is that the increasing-to-the-north magnetic gradient (see above) is evident on fig. 3a but not on Fig. 3b. This apparent regional gradient may only be a broad polarity low from deep-rooted magnetic bodies south of the Denali and Meteor Peak faults (mostly in Wrangellia, that is, but possibly including intrusive bodies in the Maclaren terrane), because it disappears when it is redistributed via pole-processing.

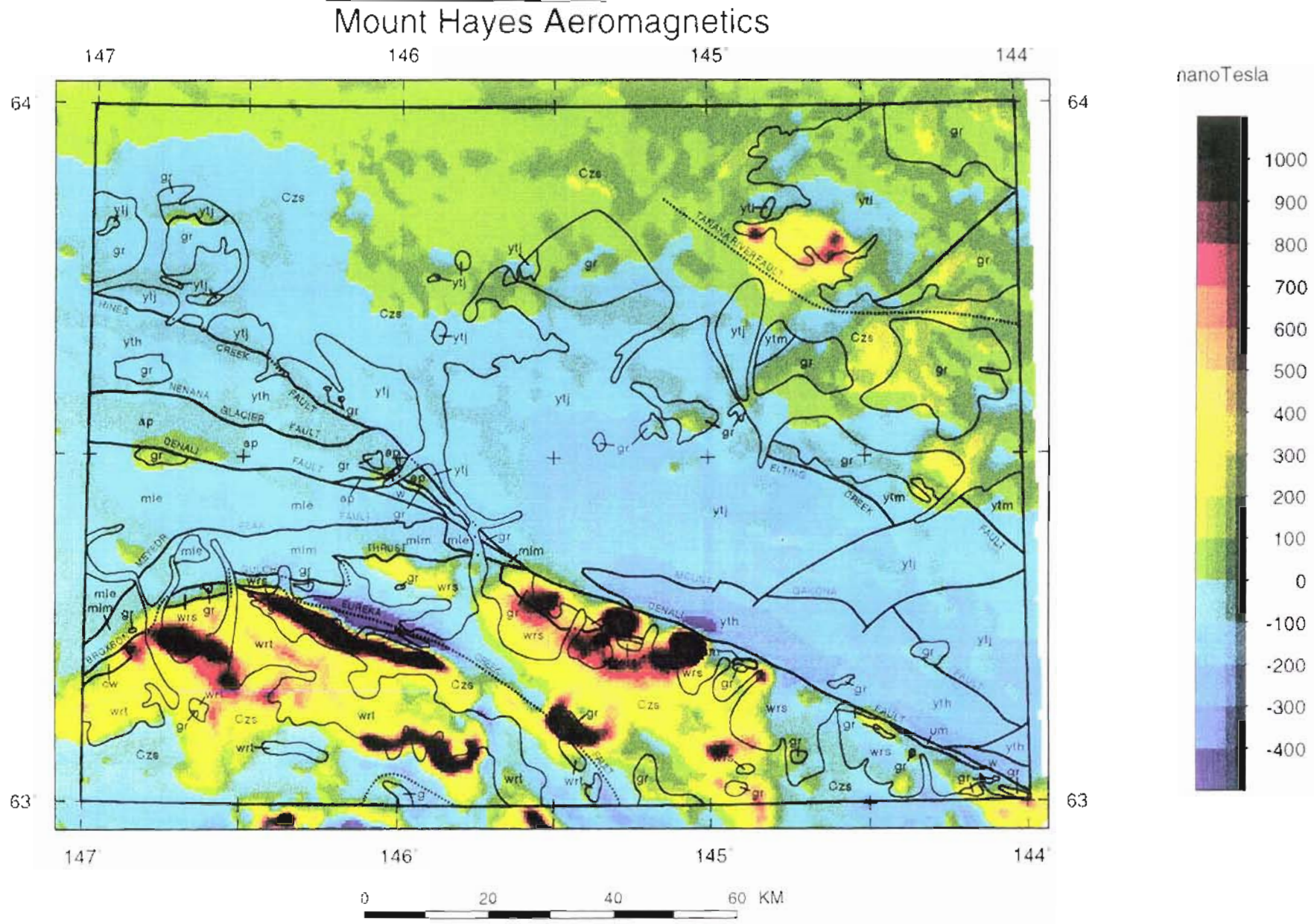

Figure 3a.--Color-shaded-relief presentation of observed aeromagnetic data, as digitized from Plate 1. Sun azimuth = 220°. Sun elevation = 60°. Using this presentation it can be seen that several geologic features that were not evident on Plate 1 nevertheless have aeromagnetic expression. Geologic overlay from fig. 2.

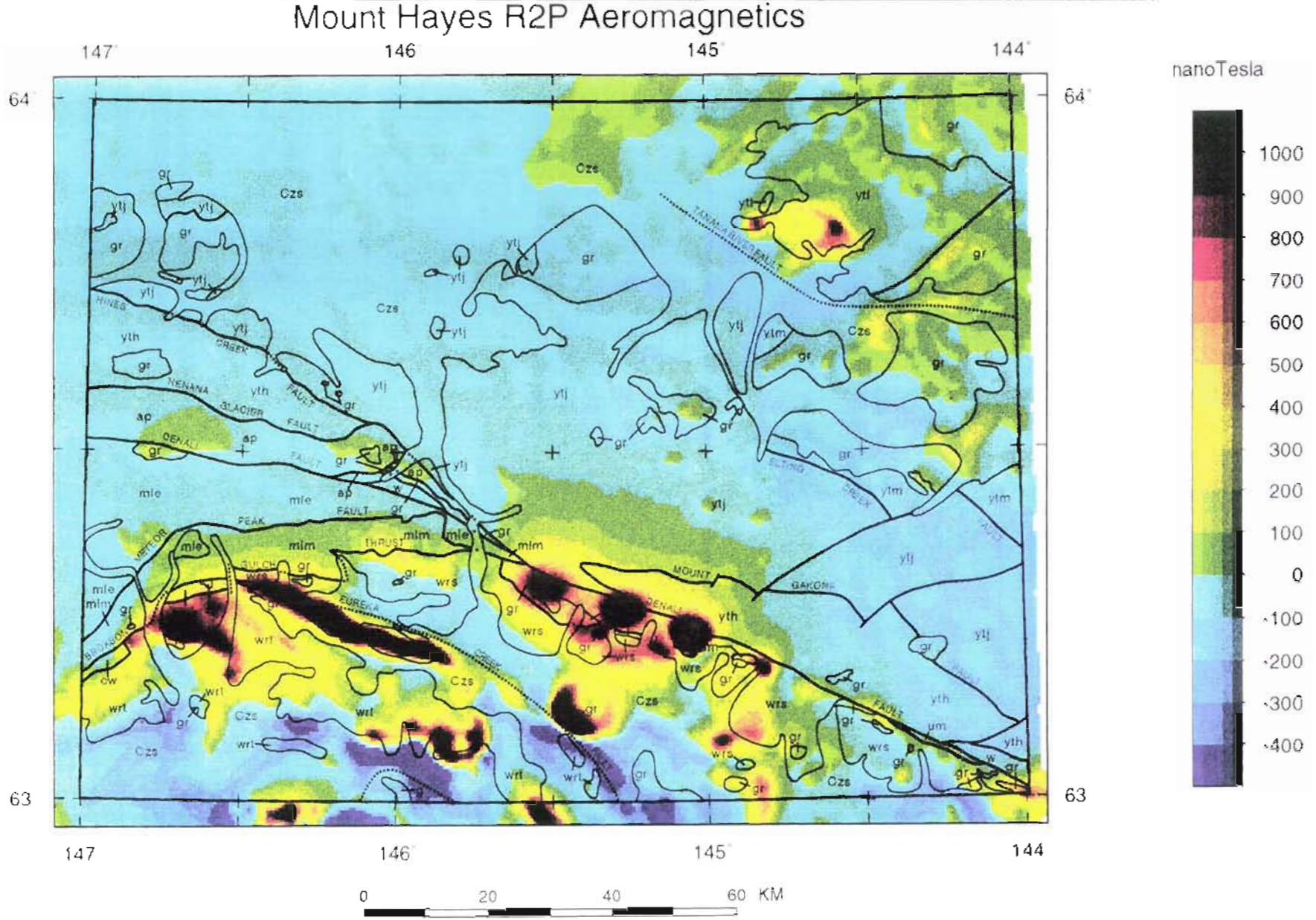

Figure 3b.--Color-shaded-relief presentation of reduced-to-pole aeromagnetic data. Sun azimuth = 220°. Sun elevation = 60°. Geologic overlay from fig. 2.

OTHER GEOPHYSICAL MAPS

Of the geophysical maps available to us, the aeromagnetic map was the most useful for helping to characterize terranes and define mineral tracts in the Mount Hayes quadrangle. However, gravity and radiometric maps and magnetotelluric data were also used, as described below. Generally speaking, gravity and aeromagnetic maps can help map geologic boundaries, estimate depth to basement beneath sedimentary or volcanic cover, and delineate igneous intrusions. Radiometric maps can help delineate areas with the elements potassium, uranium, and thorium in the near-surface rocks; high amounts of these elements can indicate and help characterize near-surface intrusive rocks. Magnetotelluric data can help to locate and characterize crustal structures.

Isostatic gravity

Fig. 4 shows isostatic gravity over the study area, as digitized from a map by Meyer and others (1996) and calculated by Saltus and others (1997). The original gravity data consisted of about 300 gravity stations measured at each milepost along the Richardson, Alaska, and Denali Highways, and at boat-accessed stations spaced a few miles apart along the Delta River and Maclaren River south of the Denali Highway. Using helicopters, gravity was measured at 63 new stations for this study. Except along the roads, however, gravity stations in the Mount Hayes quadrangle are spaced too sparsely for anything but generalized analysis. Unshaded areas in Fig 4 are more than 10 km from the nearest gravity station, and are regarded as uncontrolled. Fig. 4 shows some useful detail near roads, but it must be used cautiously everywhere else. In particular, the pattern of local highs and lows along the extreme eastern border of Fig. 4 should be discounted: the source data set included gravity stations in only a narrow buffer strip east of the Mount Hayes quadrangle, so that these features may be artifacts of the contouring program. Gravity gradients can indicate lateral density contrasts caused by tectonic boundaries, faults, or edges of regional intrusive bodies. Gravity lows can indicate sedimentary basins or felsic intrusions, and highs can indicate mafic igneous bodies, uplifted crystalline crust, or mafic crust. Isostatic gravity maps are preferred to Bouguer gravity maps for such purposes because they tend to be more sensitive to upper crustal geology (Simpson and others, 1986). If properly controlled, gravity data also can be used to get good estimates of depth to basement below surficial cover (Simpson and others, 1986; for an example in the Copper River Basin, see Campbell, 1989). Basement depths were not systematically estimated for this study.

Figure 4 shows an isostatic gravity high in the southwestern

part of the quadrangle, south of the Broxson Gulch and Eureka Creek faults. This high occurs over a sequence of ultramafic rocks in the Amphitheatre Syncline (Plate 2), and probably reflects them. Barnes and others (1991) interpreted two small gravity lows, at the north end of Summit Lake and at Donnelly Dome (see Plate 1 for locations), to reflect Tertiary basins at those places. The low at Summit Lake may be picked out on Fig 4 (contour <6 mGal, just north of the Eureka Creek fault, at about 145° 30'W). That under Donnelly Dome is not apparent on Fig 4. Barnes and others (1991) state that it is only 10 km wide from south to north, whereas its east-to-west extent is ill-defined because gravity stations are too sparse away from the Richardson Highway. Both basins were interpreted by Barnes and others (1991) to be less than about 1 km deep.

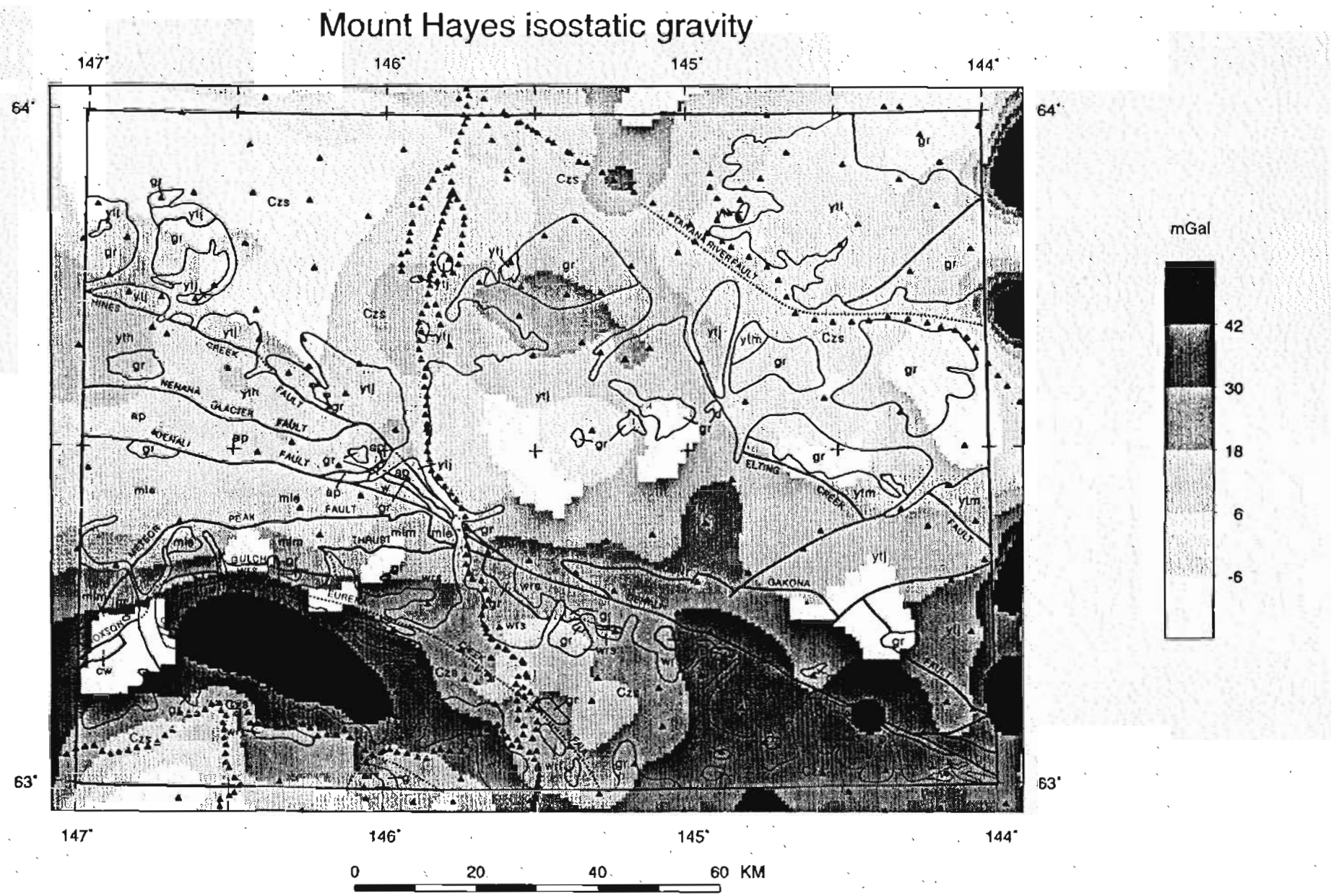

Figure 4.--Isostatic gravity map of the Mount Hayes quadrangle. Small triangles indicate gravity stations. Unshaded regions of the map are more than 10 km from a gravity station. Geologic overlay from fig. 2.

Aeroradiometrics

Under the National Uranium Resource Evaluation (NURE) Program, the Department of Energy contracted in the late 1970s and early 1980s for radiometric and magnetic surveys to be flown over much of the United States. The specifications for the NURE work were written to help sample for possible uranium deposits, not to cover all ground exhaustively. In particular, NURE surveys were flown about 150 m (500 ft) above ground level and had lines spaced 10 km (6.25 miles) apart, resulting in a nominal ground coverage of only about 4 percent (Reid, 1980). The radiometric data were collected using gamma-ray spectrometers that detected certain daughter isotopes of potassium, uranium and thorium. The resulting data are reported as percent potassium (K), and as parts per million of equivalent uranium (eU) and equivalent thorium (eTh). The designation "equivalent" is used as a reminder that the apparatus measured a daughter product in a chain of radioactive decays, and not the parent U and Th elements directly. The reported values therefore could have errors; for example, winds blowing during the survey might remove certain gaseous daughter isotopes in the decay chain. Another error arises when the survey aircraft are unable to maintain specified ground clearances over mountainous terrane. The data reduction process roughly accounts for the way gamma rays are absorbed by air, but can go wrong when ground clearances change abruptly, as in flights over rough terrain. Also, radiometric surveys sometimes seem to show basement chemistries "printing through" transported surficial material, although that should not happen -- formally, aeroradiometric data only samples approximately the upper 0.5 m (20 inches) of the Earth.

NURE spectrometric data were released on magnetic tapes, and were compiled and regridded on a 2-km grid for the state of Alaska by J.D. Phillips and F.E. Riggle of the U.S.Geological Survey (written commun., January, 1993). Maps of these data were used in preparing a mineral assessment of the state of Alaska; in particular, an assessment of south-central Alaska was done by Nokleberg, Campbell, D.P. Cox, R.J. Goldfarb, R.D. Koch, and Warren Yeend (unpublished manuscript, dated March 15, 1995). One map that Phillips and Riggle made showed pixels (rectangles about 2 km square) in which averaged potassium was especially high or low. This follows Portnov (1987), who showed that the ratio K/eTh for most rocks is in the range 0.17-0.20. If the ratio is well above that, it can indicate "potassium specialization" -- potassic igneous rocks that may relate to Au-Ag, Ag polymetallic, Mo, or Bi deposits (Hoover and others, 1992). Similarly, "thorium specialized" rocks have a much lower K/eTh ratio, and may relate to Sn, W, REE, or rare-metal deposits (Hoover and others, 1992). Phillips and Riggle (written commun., January,

1993) computed statistics for aeroradiometric data for all the state of Alaska, and set the boundaries at two standard deviations above and below averages, as follows:

Potassium specialized: K (%) > 3.0 and K/eTh > 0.275
Thorium specialized: eTh (ppm) > 10 and K/eTh < 0.095

Figs. 5-7 show eU, eTh, and K concentrations, respectively, in the Mount Hayes quadrangle subset of Phillips and Riggle's statewide compilation. Primary radiometric data for the quadrangle comes from Texas Instruments, Inc. (1978). No thorium-specialized centers occur in the Mount Hayes quadrangle, but that there is an area in the extreme southeast corner of the quadrangle that is highly potassium-specialized. This potassium-specialized area apparently is centered on the Slana mining district, which lies immediately south of the southern border of the Mount Hayes quadrangle, along the Slana River valley (Plate 1). Except for the Slana district, quadrangle rocks south of the Denali and Hines Creek Faults are relatively low in K, eU, and eTh, and rocks north of the these faults (the Yukon-Tanana terrane, in other words) are relatively higher. As might be expected, higher radioelement concentrations occur near outcrops of rocks of the Yukon-Tanana terrane and associated intrusions into it, and lower concentrations occur where these source rocks are covered by glacial- and fluvial-transported sedimentary deposits.

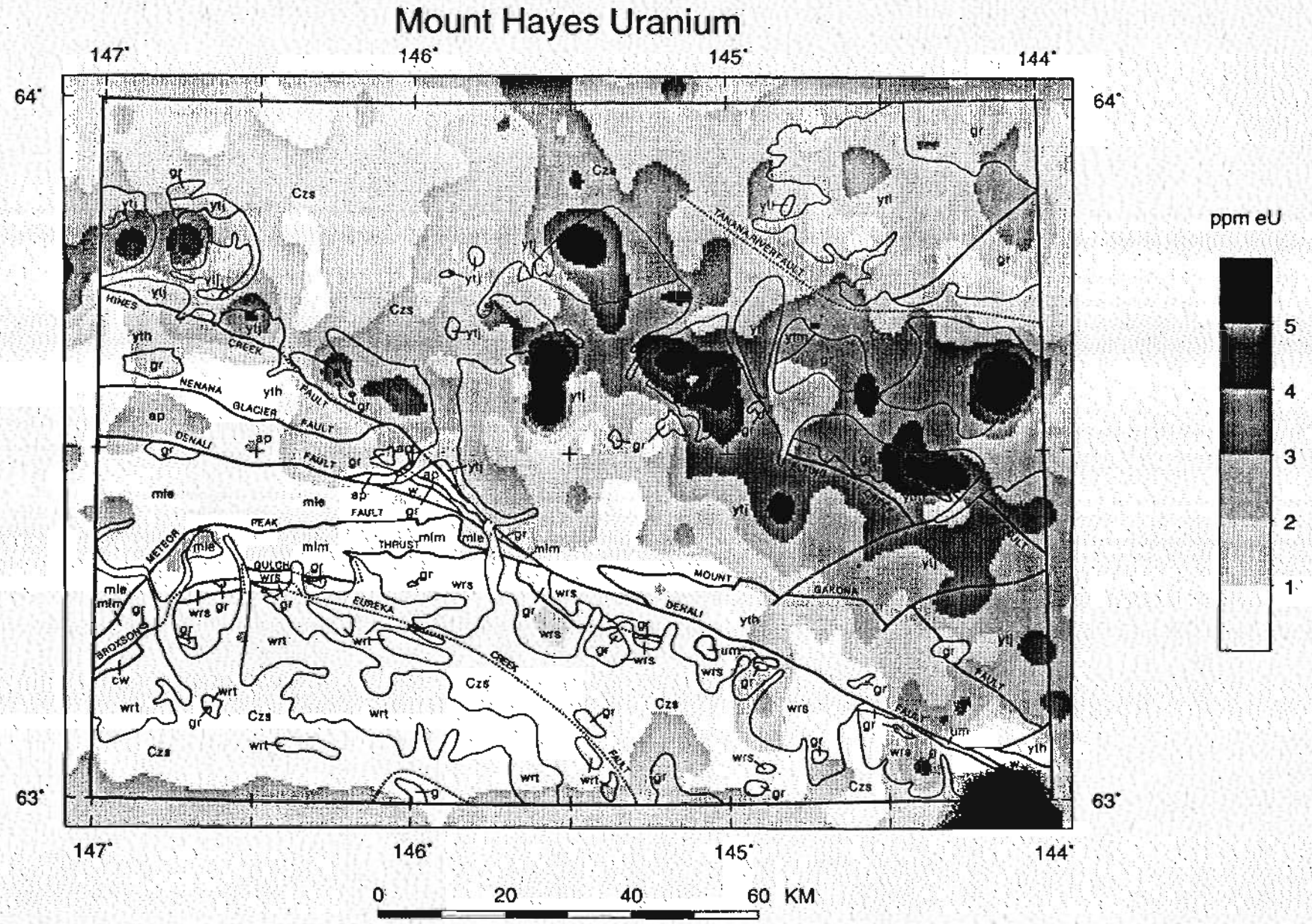

Figure 5.--Aeroradiometric map of the Mount Hayes quadrangle, showing concentration of equivalent Uranium (eU). Geologic overlay from fig. 2.

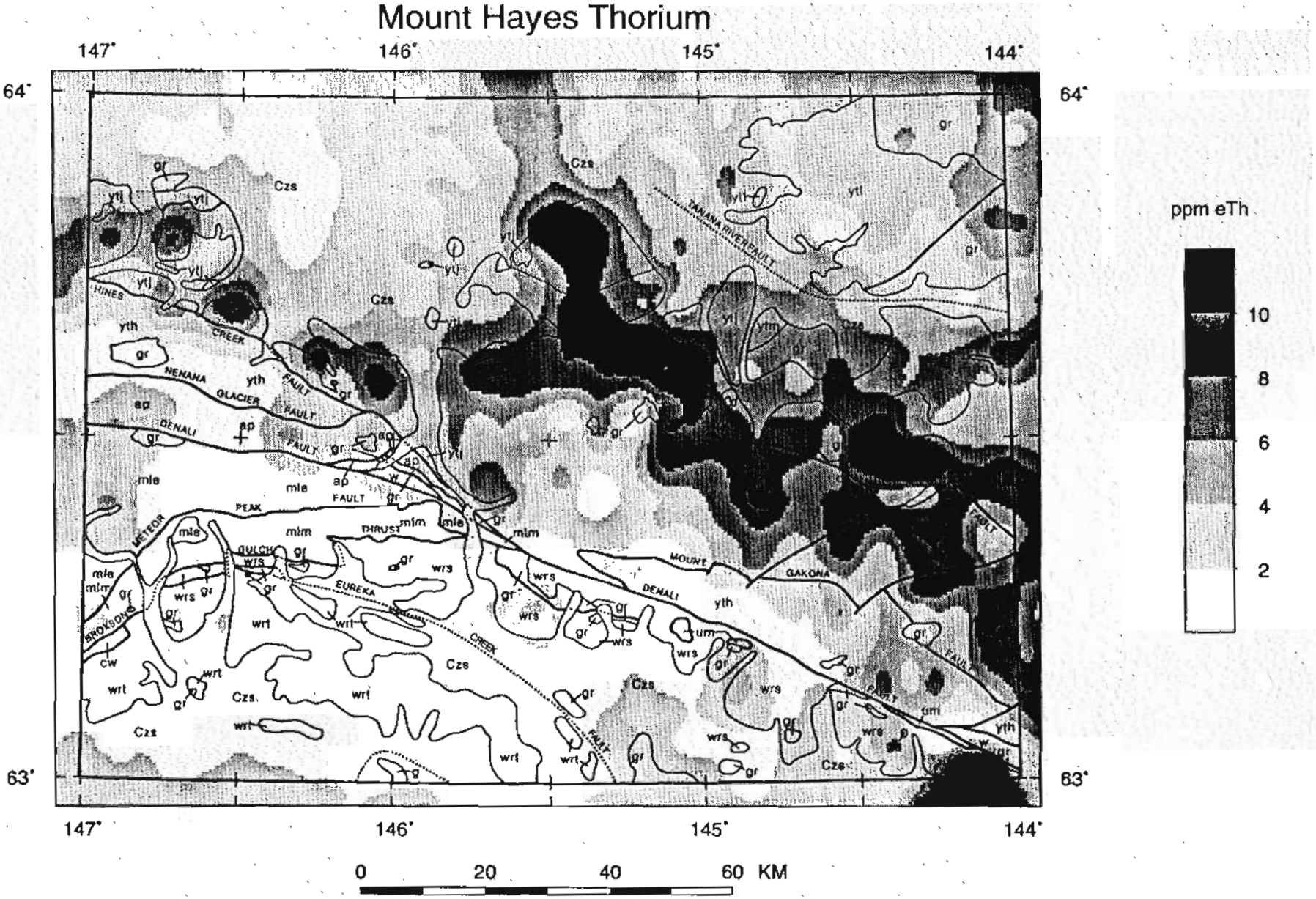

Figure 6.--Aeroradiometric map of the Mount Hayes quadrangle, showing concentration of equivalent Thorium (eTh). Geologic overlay from fig. 2.

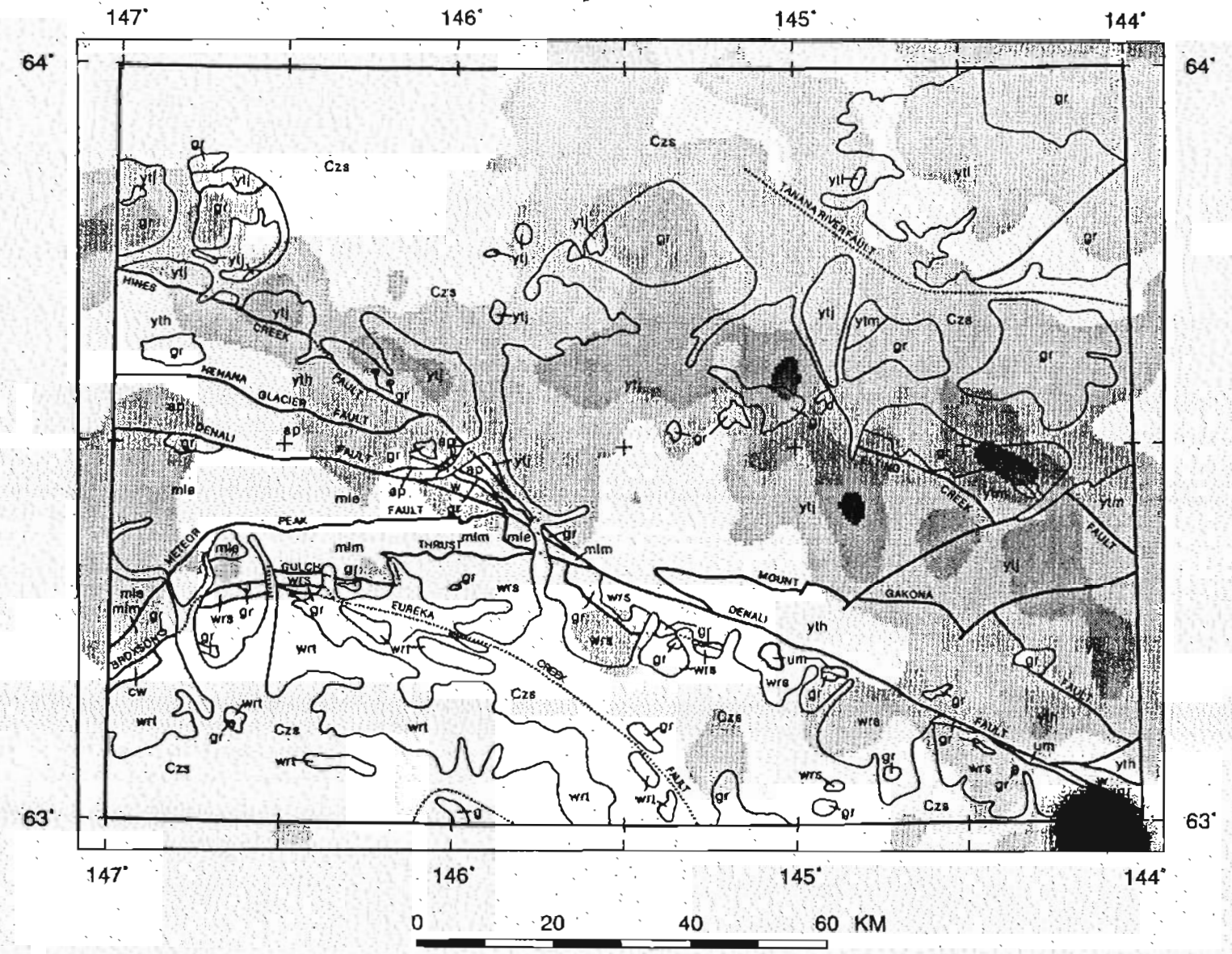

Figure 7.--Aeroradiometric map of the Mount Hayes quadrangle, showing concentration of Potassium (K). Geologic overlay from fig. 2.

Magnetotelluric soundings

During 1985-1990, USGS made more than 300 magnetotelluric (MT) and audio-magnetotelluric (AMT) soundings in Alaska along the Alyeska pipeline corridor as part of the Trans-Alaskan Crustal Transect (TACT). The MT method measures electrical conductivity of the crust and upper mantle. The AMT method is similar, but only investigates to depths of several km; AMT is operationally faster than MT, and so was used to fill in between primary MT stations along the Transect. Figure 8 shows the locations of 83 MT soundings and 20 AMT soundings made within the Mount Hayes quadrangle. These soundings have been discussed by Stanley and others (1990) and by Labson and Stanley (1989). The MT/AMT work shows that the crust just to the north of the Denali Fault is electrically conductive at depths of 5-15 km. This point is further discussed along with fig. 10, below.

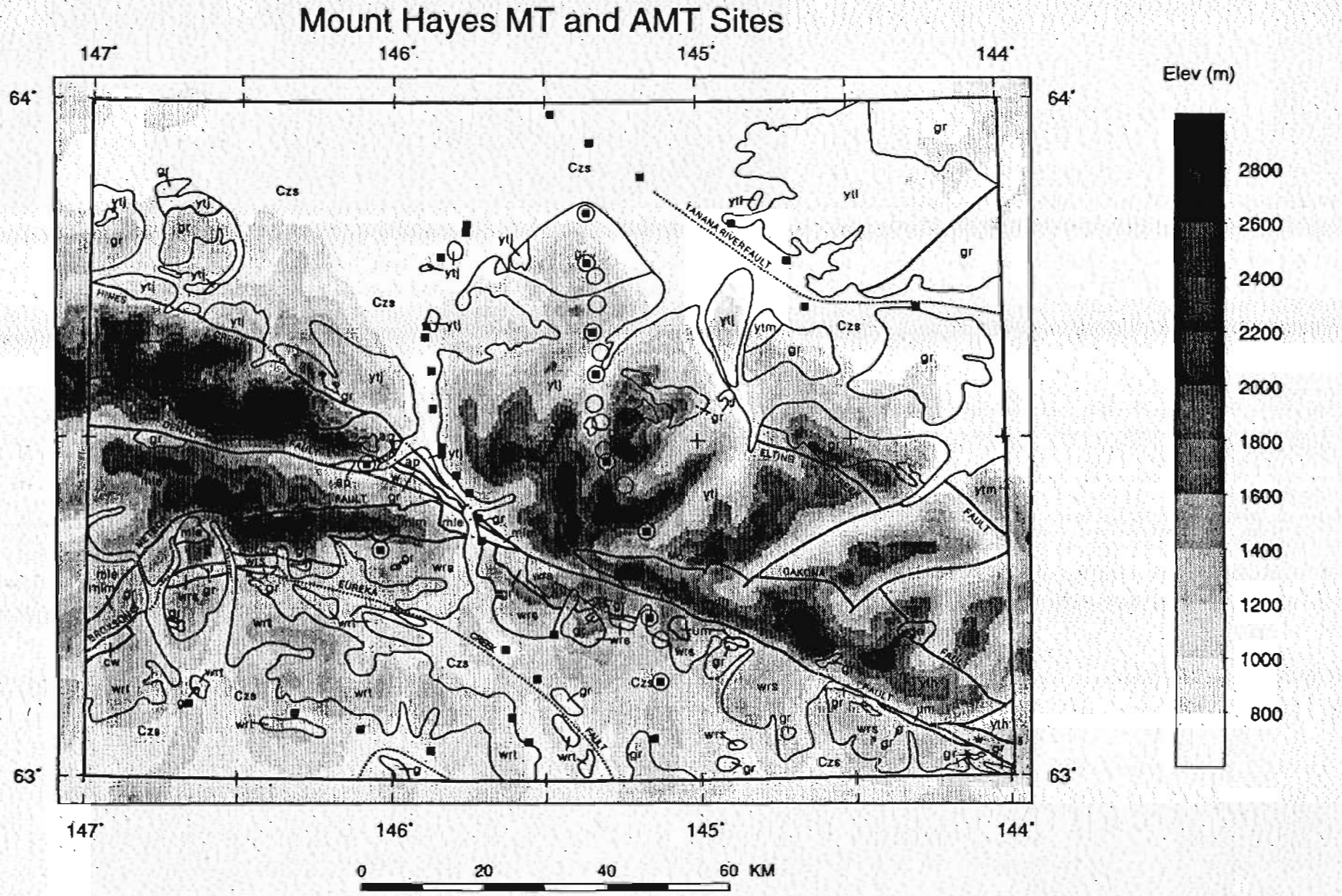

Figure 8.--Locations of MT (heavy squares) and AMT (open circles) soundings in the Mount Hayes quadrangle. Background shading patterns show topographic elevation. Geologic overlay from fig. 2.

MEASURED MAGNETIC SUSCEPTIBILITIES OF ROCKS

The ratio relating the magnitude of the induced magnetization vector in a sample to the magnitude of the magnetic field vector which causes it (the Earth's field, for example) is the "susceptibility" of the sample, and is typically a few parts per thousand. Though susceptibility is a dimensionless quantity, there are two systems of reporting in use, so that it is necessary to note whether "c.g.s." or "S.I." system was used (1 c.g.s. unit = 12.57 S.I. units). Using a small hand-held meter, susceptibilities of many outcrops were measured in the field during the 1982 field season in an attempt to identify source rocks for various features on the aeromagnetic map. Only the induced component of rock magnetism is indicated thereby, and there may be an additional remanence which boosts the net magnetic fields due to the body. Most rocks with high remanence, however, will also show high susceptibility on the meter.

During the summers of 1982 and 1984, magnetic susceptibilities were measured using a Scintrex SM-5 meter of many rock outcrops in the Mount Hayes quadrangle (Table 1). The SM-5 meter could not measure susceptibilities below 1 x 10^{4} cgs (=126 x 10^{-5} S.I.), so that susceptibilities of any rocks below this threshold are marked "<126" (x10^{-5} S.I.) in the table. Rocks having such low susceptibilities are unlikely to cause significant aeromagnetic anomalies. During the summer of 1985, a few more outcrops were measured using a GeoInstrument JH-6 meter with a more sensitive threshold of about 1 x 10^{-5} S.I.

In most cases, only a few outcrops of each rock type were measured, and it is not known how representative the measured susceptibilities are of the whole rock unit. Only three rock units had enough measurements to make histograms of the results (fig. 9). Units of Slana Spur Formation (PPs on Plate 2) and pelitic schist of the Jarvis Creek Glacier subterrane (jcs on Plate 2) were measured using a SM-5 meter at 5 m intervals on outcrops along the Richardson Highway to get the values shown. As a very approximate rule, rocks with susceptibilities less than about 500 x 10^{-5} S.I. are unlikely to cause anomalies on aeromagnetic maps like Plate 1. Hence, unit jcs is assessed as "nonmagnetic", at least so far as likely aeromagnetic signatures are concerned. Similarly, unit PPs is largely nonmagnetic, but contains magnetic subunits. If such subunits are large enough, they could cause anomalies on aeromagnetic surveys.

Table 1.--Magnetic susceptibilities measured on outcrops in and rock samples from the Mount Hayes quadrangle and closely adjacent quadrangles. Terrane abbreviations from fig. 2.

Quad	Location	Terrane	Lithology	Susc (x 10^{-5} S.I.)	Comments
A1	T15N,R6E,S23	um	peridotite	3800	
A4	T21S,R10E,S23	wrt	gabbro	<126	
A5	T19S,R9E,S28	wrt	metagabbro	500-750	
--	--	--	serp. mafic	5000	
--	--	--	pyrox. cumulate	250	
--	--	--	greenstone	370-5000	
A5	T21S,R5E,S4	wrt	Nikolai	<126-5800	
A5	T21S,R8E,S1	wrt	Nikolai	<126	
A6	T19S,R5E,S32	wrt	quartz diorite	880	Massive sulfide prospect
--	--	--	limestone	<126	
--	--	--	skarn	250	
--	--	--	diorite	630-8800	
A6	T20S,R4E,S1	cw	greenstone schist	<126	
A6	T20S,R4E,S11	cw	metagabbro	<126	
A6	T20S,R5E,S6	cw	greenstone volc.	<126	
B4	T18S,R11E,S21	wrs	granodiorite	80	Rainbow Mountain granitic pluton
C2	T21N,R16E,S8	ytm	granitic rock	<126	
C3	T20N,R14E,S3	ytj	granodiorite	<126	Mt. Hajdukovich alkalic gabbro
--	--	--	amygd. dacite	1900	
--	--	--	fine gr dacite	3300	
C3	T14S,R12E,S35	ytj	schist	<126	
C3	T15S,R12E,S2	ytj	schist	<126	
C6	T14S,R5E,S32	ytj	pyrite schist	<126	Miyaoka massive sulfide occurance
Healy	T13S,R2E,S28, S29,31	ytj	pyroxine granodiorite	126-500	Buchanan Creek pluton
Healy	T13S,R2E,S22	ytj	serpentine	750	
--	--	--	schist	<126	
Nabesna	T8N,R3E,S??	wrs	Tetelna volcanic	30-3000	

The rock unit in the Mount Hayes quadrangle whose magnetic properties has been best studied is the Nikolai Greenstone. Hillhouse and Gromme (1984) measured paleomagnetic poles in Nikolai Greenstone from 7 sites in or closely adjacent to the quadrangle (Plate 2), finding that Wrangellia was located at a far lower geomagnetic latitude in late Triassic time than at present. J.W. Hillhouse (written commun., April, 1986) provided susceptibility and natural remanent magnetization (NRM) data for most of his Nikolai Greenstone samples, and from these we calculated the "effective susceptibility" values shown in figure 9d and the total magnetization directions given in table 2. Effective susceptibility and total magnetization include both induced and permanent magnetization components, and so are of more value for analyzing aeromagnetic data than susceptibility

measurements alone. The results for the Nikolai Greenstone show that effective susceptibilities are greater than true susceptibilities, and that total magnetization direction at some sites (particularly sites 6 and 7, in the Slana River subterrane) deviates substantially from that of the Earth's field. However, the Nikolai Greenstone is relatively thin at sites 6 and 7, and the resulting effects as seen on the aeromagnetic map are not substantial. Luckily, total magnetization directions at sites in the Tangle subterrane, where the Nikolai Greenstone is thicker, are approximately aligned with the Earth's field direction; there our analysis can use an effective susceptibility without taking deviant magnetization directions into account.

Table 2.--Mean magnetic properties for Nikolai Greenstone samples from sites 1-7, calculated from data supplied by J.W. Hillhouse (written commun., April 1986). Sites 1 and 2 were in the Clearwater Mountains in the Healy A-1 quadrangle at 63.09° N, 147.38° W and 63.12° N, 147.11° W, respectively. Other sites are shown on Plate 2. Properties were not measured for the samples from Site 3. N = number of samples measured from the site. Both true and effective susceptibilities are in S.I. units x 10^{-5}. Q (Koenigsberger ratio) is the ratio of permanent to induced magnetization; higher values mean stronger permanent magnetism components. Values are referred to Earth's field of magnitude 56,400 nT, declination 28°, and inclination 76°.

Site	N	True Susc.	Q	Effective Susc.	Declination (deg)	Inclination (deg)
1	13	2701	0.431	4125	22.69	67.45
2	13	2265	0.542	3406	52.81	66.36
4	73	76	0.143	117	24.88	74.99
5	18	788	1.929	2891	59.38	71.93
6	43	984	1.320	3458	70.36	45.67
7	60	358	1.443	2090	83.74	51.21

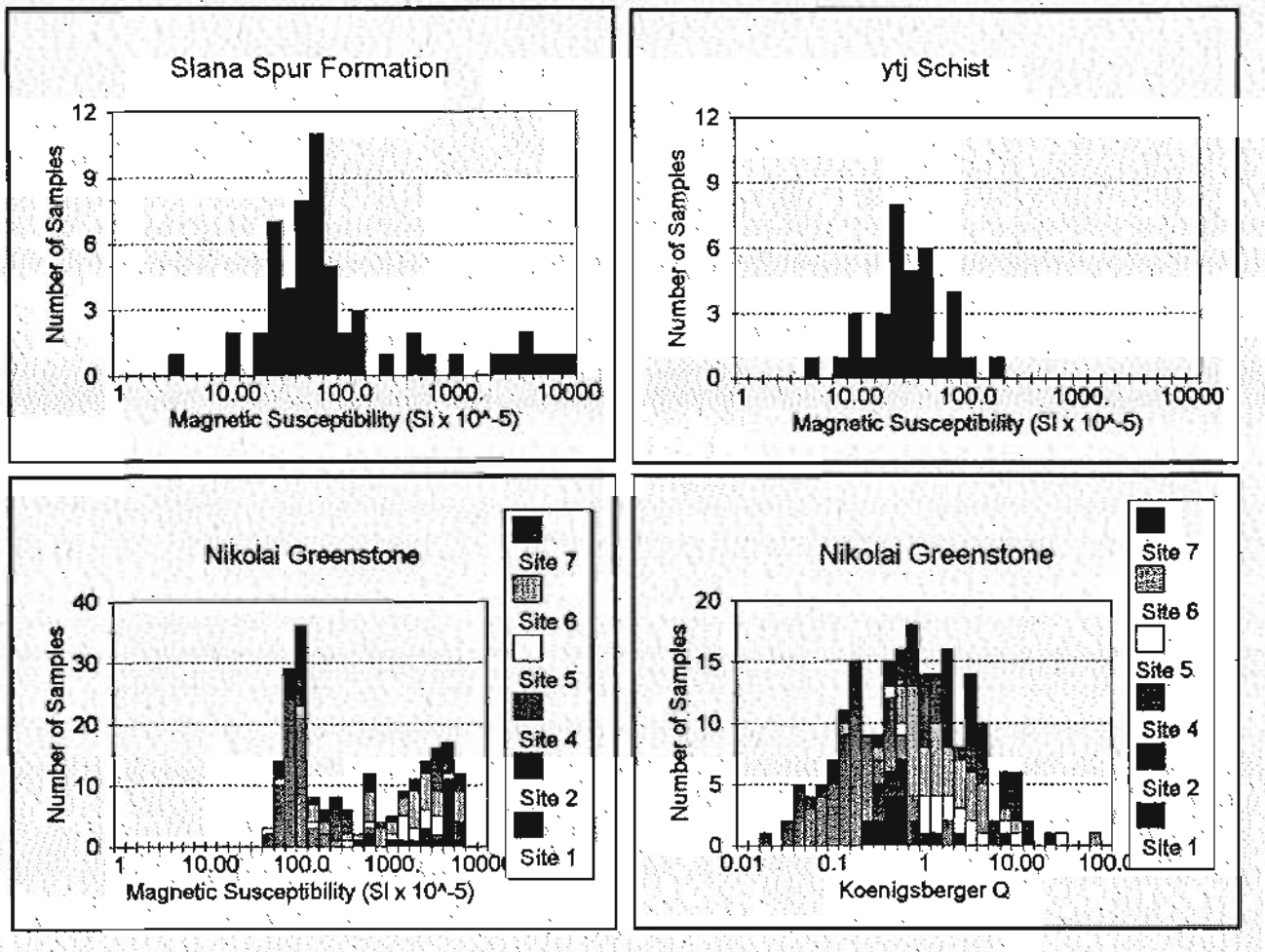

Figure 9.--Histograms showing distribution of measured magnetic susceptibilities for Slana Spur Formation rocks, metasedimentary schist of Jarvis Creek Glacier subterrane ("ytj schist"), and Nikolai Greenstone. Distribution of Koenigsberger Q values for Nikolai Greenstone are also shown. Nikolai Greenstone sample sites are plotted on Plate 2. Sites 1 and 2 are in the adjacent Healy quadrangle. Site 4 samples were not calculated. Data for Nikolai Greenstone were provided by J.W. Hillhouse (written commun., 1986).

PROMINENT AEROMAGNETIC FEATURES

The Mount Hayes aeromagnetic map (Plate 1) is divided grossly into two magnetic provinces, a "quiet" magnetic province of low-amplitude, long-wavelength magnetic features to the north, and a "noisy" magnetic province of high-amplitude, short-wavelength features to the south. The concave-south boundary between these two magnetic provinces is a fundamental one in the area, representing the Denali fault on the east, the Broxson Gulch fault on the west.

Magnetic anomalies in the northern magnetic province are generally rounded, intermediate-wavelength, low-amplitude features which can indicate buried plutons. Some anomalies have straight edges ("magnetic lineaments") which may reflect faults. Some of these magnetic lineaments in the northern magnetic province trend northeast. Magnetic lineaments in the southern magnetic province dominantly trend west-northwest.

In the western portion of the southern magnetic province there are a number of continuous, west-northwest trending magnetic highs that reflect high-susceptibility units. The elongated shapes suggest the source bodies here may be tabular. In the eastern portion of the southern magnetic province the strong magnetic highs are more rounded, suggesting more equidimensional source bodies, probably plutons. Finally, in both eastern and western portions of the southern magnetic province there are many short-wavelength, lower-amplitude "birds-eye" magnetic patterns that are typical of extrusive volcanic rocks, in this case the Nikolai Greenstone and other volcanic rocks (possibly including Paleozoic ones?) of the Wrangellia terrane.

MAGNETIC CHARACTER OF TECTONOSTRATIGRAPHIC TERRANES

Hayes Glacier, Jarvis Creek Glacier, Macomb, and Lake George subterranes of the Yukon-Tanana terrane

The Hayes Glacier subterrane of the Yukon-Tanana terrane is generally nonmagnetic in character, but contains several small, rounded or west-northwest-trending linear magnetic highs. The inferred source bodies (near anomaly 1, Plate 2) are magnetically similar to bodies inferred for the Jarvis Creek Glacier subterrane, and may represent small plutons emplaced after the two terranes were sutured together.

The Jarvis Creek Glacier subterrane of the Yukon-Tanana terrane is characterized by "magnetic measles" -- local, rounded magnetic highs of 10 or 20nT amplitude that occur over topographic highs. Measles are generally an artifact of the data gathering process and have no geological significance. They are caused when the sensor of the survey instrument comes closer than usual to the ground, usually over sharp ridges or peaks, and so

sees a slightly higher field there. There is no reason to suppose hilltops in the Jarvis Creek Glacier subterrane are particularly different from other places; therefore, we infer that the mainly medasedimentary schists of the Jarvis Creek Glacier subterrane are weakly magnetic everywhere. The widespread occurrence of these measles reinforces the impression of magnetic uniformity for the unit. West of approximately the Richardson Highway (Plate 1), there are fewer and smaller hills in the Jarvis Creek Glacier subterrane and the unit is covered by surficial deposits. Here the measles disappear.

Besides magnetic measles, the Jarvis Creek Glacier subterrane contains many small bodies (under anomalies 2 on Plate 2) which probably represent near-surface, moderate-susceptibility, mainly-Cretaceous granitic plutons. Some of these bodies occur near areas of known volcanogenic massive sulfide deposits, but it may be that this association is not genetic and only reflects accidental juxtopositions. Of particular interest to the explorationist are magnetic "horsehoes", rings of magnetic highs with centered or reentrant lows. Such magnetic features may be due to porphyry systems, in which a later intrusion into an earlier, more magnetic pluton alters or destroys preexisting magnetic minerals (Cunningham and others, 1984). Such a horseshoe anomaly occurs over a granite pluton which cuts the Mount Gakona fault between Jarvis Creek Glacier and Hayes Glacier subterranes. The inferred source body (under anomaly 3) is marked "Rumble Creek body" on Plate 2.

Another horseshoe anomaly occurs over the Mt. Hajdukovich (Plate 1) alkalic gabbro complex. In addition to porphyry systems, magnetic horseshoe anomalies may be due to carbonitite intrusions, to ring dike systems, or to plutons whose magnetic minerals have frozen early in the reaction series of cooling and so are concentrated near its outer edges. Such a pluton must subsequently have been uplifted and any magnetic cap removed by erosion. The Mt. Hajdukovich pluton (under anomaly 4) appears to be of this latter type. The source rocks are monzonite and alkali gabbro with magnetic susceptibilities of 11,000-32,000 x 10^{-5} S.I. These rocks had the highest susceptibilities measured in the quadrangle.

In the northwestern portion of Plate 2 there are three elongated, east-west trending, low-amplitude magnetic highs in the Jarvis Creek Glacier and Hayes Glacier subterranes. The northernmost, anomaly 5, is near Molybdenum Ridge. The source rock for the "Molybdenum Ridge Body" (Plate 2) is inferred from outcrops to be quartz monzonite. The second, anomaly 6, trends westward from near the mouth of Hayes Glacier. Its source rock is not known. The third, anomaly 7, may reflect several nearby medium- to high-susceptibility bodies. One of these is the "Mount Skarland pluton" (Plate 2), an inferred plum-shaped pluton

of metagabbro in the Hayes Glacier subterrane that lies under the eastern flank of Mount Skarland. Its source rocks do not crop out.

The Macomb subterrane is characterized by local magnetic highs, probably due to mainly Cretaceous dikes and small plutons. Highs on the Macomb Plateau, and to the east and southeast, appear to be due to small bodies and to a shallow granitic batholith ("Macomb Plateau batholith", under anomaly 8 on Plate 2). The anomalies over the Macomb Plateau batholith have much high frequency detail, forming the "birdseye" type of patterns which often characterize volcanic flows. Here, however, there are no known flows. Thus, the source body is inferred to be a shallow quartz monzonite intrusive unit which crops out in scattered places on the Macomb Plateau. In order to produce the observed magnetic birdseyes, the inferred batholith must have variable susceptibility, variable depths to its top, or both. The Macomb terrane also contains two east-west trending inferred dikes (under anomalies 9 on Plate 2), that are correlated with known dikes of diorite or granodiorite.

The Lake George subterrane is characterized by a large magnetic high (anomaly 10, over the "Lake George body" of Plate 2), and by large patches of magnetic birdseyes indistinguishable from those of the Macomb terrane. At depth the Lake George body seems to extend 10-15 km farther southwest from the most southerly outcrops of granitic rock. As in the Macomb terrane, magnetic source bodies in the Lake George terrane are interpreted as shallow, variable granitic plutons, possibly of quartz monzonite or granodiorite, of mainly Cretaceous age.

Many mapped and inferred faults in the Yukon-Tanana terrane, such as the Tanana River fault, the Elting Creek fault, the West Fork fault, and the Robertson River fault (Fig. 2; Plate 2), have no magnetic expression. There is, however, a strong magnetic lineament, labeled the "Sand Creek lineament" on Plate 2, which may represent a fault trending northeast from near Mt. Hajdukovich to Sand Lake and down Sand Creek. The Sand Creek lineament is not offset by the Tanana River fault. A ground traverse across the Sand Creek lineament was made to the east of Horn Mountain, but no high or intermediate susceptibility rocks were found there. Probably a relatively magnetic body just northwest of the Sand Creek lineament (under anomaly 11) is buried at that place.

Aurora Peak and Windy terranes

Like the Yukon-Tanana terrane to the north, the Aurora Peak and Windy terranes consist largely of non-magnetic rocks, and so cannot be distinguished magnetically. Even such a major subterrane boundary as the Hines Creek fault has little magnetic expression, except for a short magnetic lineament where it trims

a buried magnetic body near the Trident Glacier. The Aurora Peak and Windy terranes are intruded from place to place by relatively linear, west-trending, intermediate susceptibility inferred buried granitic plutons. Some of these inferred plutons appear to straddle terrane boundaries. One such inferred pluton or complex of plutons (the "Aurora Peak Body", under anomaly 12 on Plate 2) occurs in a wedge between the Denali fault and Hines Creek fault without clearly belonging to any of several terranes that are juxtaposed there. Another such inferred pluton is the intermediate-susceptibility body or complex of bodies under anomaly 13 in the divide between Black Rapids and Susitna Glaciers. Quartz monzonite crops out south of the Denali fault under anomaly 13's strongest high, but much of anomaly 13 lies across the Denali Fault to the northeast. At least three explanations for this northward extent of anomaly 13 are possible: (a) this segment of the Denali Fault may dip northward at a shallow angle; (b) the intrusion may have been emplaced after the most recent movement on this segment of the Denali Fault; and/or (c) the Denali fault merely may juxtapose two relatively magnetic bodies at this place. This point is further discussed with figure 10, below.

Maclaren and Clearwater terranes

Like the Jarvis Creek Glacier subterrane of the Yukon-Tanana terrane, the Maclaren terrane displays magnetic measles from place to place on Plate 1, so we infer rocks of intermediate-to-low susceptibility there. There are three inferred magnetic plutons in the Maclaren terrane, including the inferred quartz monzonite pluton discussed above (under anomaly 13) which appears to straddle the Denali fault. The other two inferred plutons probably intrude rocks of the East Susitna batholith, but apparently do not crop out. The larger of the two (the "East Fork Body", anomaly 14 on Plate 2) has a horseshoe-shaped anomaly pattern whose cause is unknown. Its reentrant low occurs over a small stream which drains northward into the glacial headwaters of the East Fork of the Susitna River. Additional detailed work is needed to determine whether a porphyry system might be present.

Anomaly 15 is a strong magnetic high southeast of the headwaters of Clearwater Creek, which straddles the northwestern boundary of the Clearwater terrane. Quartz monzonite rocks crop out there.

Wrangellia terrane and terrane of ultramafic and associated rocks

The Wrangellia terrane contains many intermediate-to-very-high susceptibility rocks, including (in approximate order from high to low susceptibility) olivine- and pyroxene-cumulate igneous rocks, gabbros, Nikolai Greenstone, and granitic

intrusive rocks (table 1). There appear to be two magnetic subprovinces in the Wrangellia Terrane, approximately corresponding to the Tangle and Slana River subterranes of Nokleberg and others (1982). The two magnetic subprovinces are divided along a series of magnetic lineaments that follow the Eureka Creek fault. This series of magnetic lineaments passes through the southern edge of Plate 2 at about 145° 25' W. At about that point, they appear to join a lineament ("the Drum lineament" of Campbell, 1986) that continues south-southeast on aeromagnetic maps of the Gulkana quadrangle (Andreasen and others, 1964; U.S. Geological Survey, 1985) to at least the vicinity of Mount Drum in the western Wrangell Mountains.

The magnetic subprovince southwest of the lineament (the Tangle subterrane, approximately) has strong magnetic features (anomalies 16) probably due to thick sheets of cumulate intrusives and extrusive source bodies. These cumulate rocks may form the floor of the Amphitheatre syncline. In this area also are numerous magnetic measles which occur over thick sequences of subaerial basalt flows of the Nikolai Greenstone. These Nikolai Greenstone magnetic signatures, however, only modulate and locally enhance the magnetic fields due to much more extensive bodies at depth. To the northeast of the lineament (the Slana River subterrane, approximately) there are strong magnetic features probably due to large intrusions and to smaller local plutons. The northwesternmost prong of the Slana River subterrane, extending into Maclaren terrane in the general area between the Delta River and Broxson Gulch, has a complex magnetic signature with local lineaments and birdseyes. At least some of its source rocks (such as under anomaly 17) appear from sparse outcrops to be olivine cumulate and other ultramafic rock.

Anomaly 18 in the north-central portion of the Slana River subterrane is a large, strong magnetic high which probably reflects a large intrusive body ("Gakona Glacier body" on Plate 2, formerly the Gulkana batholith of Campbell and Nokleberg, 1985). Four major magnetic highs are marked whose source bodies may represent cupolas on this large intrusive body or individual plutons within it; the "Rainbow Mountain subbody", the "Icefall Peak subbody", the "Ultramafic subbody", and the "Chistochina Glacier subbody". The Rainbow Mountain area is clearly underlain by a large magnetic body, but the source rock type is not known. The smooth unbroken magnetic signature argues against porphyry-type mineralization here, since alteration associated with porphyries usually destroys magnetic minerals. The source of the Icefall Peak magnetic high is also unknown, but must be a similar large magnetic body at depth. The Ultramafic subbody high is due at least partly to a relatively thin, fault-bounded block of ultramafic rock there. All of this area has complex structure, including the eastern end of the Broxson Gulch thrust

and several branches of the McCallum Creek-Slate Creek thrust. Possibly the present surface rocks were thrust over a pre-existing magnetic pluton along some of these faults. The strong magnetic signature indicates the tops of these bodies are quite near the surface, arguing either that the thrust sheet capping the magnetic cupolas is thin or that the bodies intruded after thrusting took place. The northern edge of the inferred large intrusive body, however, is neatly trimmed by the Denali Fault; at least some movement on this segment of the Denali Fault happened after emplacement of the Gakona Glacier body(see Profile A-A', below).

If the Gakona Glacier body was broken by the Denali fault, where is its other part? One possibility is the Klein Creek pluton in the McCarthy, AK, quadrangle, a large magnetic body discussed by Case and MacKevett (1976). Like apparent outcrops of the Rainbow Mountain body, the Klein Creek pluton is composed of diorite, hornblende biotite granodiorite, and quartz monzonite (Case and MacKevett, 1976; MacKevett, 1978). The Klein Creek pluton was emplaced about 111 Ma (Richter and others, 1975); a sample collected from the Rainbow Mountain body also has an age of 111 Ma (Nokleberg, Aleinikoff, Dutro and others, 1992). The magnetic signature of the Klein Creek pluton appears to be trimmed on the south for about 55 km by the Totschunda fault; that of the Gakona Glacier body is trimmed on the north for about 45 km by the Denali fault. To match these two edges, we must suppose about 220 km of displacement along the Totschunda fault and an additional 40 km of displacement along the Denali fault has taken place in the last 111 m.y. Units intruded by the respective plutons have been shown to be broadly correlative (Richter and Dutro, 1975): for example, the Permian Hasen Creek Formation (MacKevett, 1978) correlates with the Permian Eagle Creek Formation, and the Permian-Pennsylvanian Station Creek Formation (MacKevett, 1978) with the Permian-Pennsylvanian Slana Spur Formation (Nokleberg and others, 1994).

South of the Gakona Glacier body, near Gunn Creek, there is a horseshoe-shaped anomaly pattern with an angular reentrant low (anomaly 19). This low has very steep sides, suggesting either post-intrusion faulting of a curious pattern, or successive intrusions into an earlier pluton which destroyed magnetic minerals there. The source body ("Gunn Creek Body" on Plate 2) is inferred from local outcrops to be a granodiorite. Further detailed work over the reentrant magnetic low near the intersection of Gunn Creek and the stream from Gunn Lake is needed to determine if a porphyry system is present there.

There is a north-trending lineament at approximately the Chisna River ("Chisna River lineament" on Plate 2) separating a region of low magnetic fields on the east from one of higher fields on the west. The lineament is parallel to flight line

direction, so it is not well-controlled. It does not correspond in detail to any mapped bedrock contact. The Chisna River lineament appears to correlate with a geochemical transition, however, as measured by stream sediment and rock-geochemical samples (Curtin and others, 1989).

Of the many magnetic highs just west of the Chisna River lineament, the northernmost (anomaly 20) is quite rounded, and may reflect a mapped pluton ("Chistochina Glacier subbody" on Plate 2). This pluton consists of coarse-grained hornblende diorite, which grades downward within 1000 ft to a magnetite-rich diorite (I.M. Lange, oral commun., 1984). In addition, part of anomaly 20 undoubtedly is caused by a thin slice of ultramafic rocks that is thrust over the pluton tp the south.

Some magnetic highs just west of the Chisna River lineament are elongated to the east, suggesting tabular source bodies. The Chisna River lineament may represent a fault, for it seems to cut off these east-trending, elongated magnetic highs. Alternately, these highs may reflect additonal cupolas on a deep portion of the Gakona Glacier body, or a series of smaller, local plutons. Most of the source bodies are buried or at least obscured by surficial glacial debris or Nikolai Greenstone flows, but some highs appear to occur over sparse outcrops of gabbros. Other gabbro bodies, with accompanying magnetic highs, also crop out nearby. Two of these bodies are just east of the Chisna River lineament, near the headwaters of Red Mountain Creek and Rock Creek, respectively (separate peaks on anomaly 21). Another body is farther to the west, just south of Caribou Lake (anomaly 22). The gabbro south of Caribou Lake crops out along a west-trending, linear magnetic high. There is a similar linear high north of Caribou Lake (anomaly 23) whose source rock is unknown.

The region of subdued magnetic fields to the east of the Chisna River lineament corresponds partly to non-magnetic sedimentary and volcanic formations such as the Eagle Creek Formation and Tetelna Volcanics. There are three strong magnetic highs in this region of otherwise low fields whose sources have been identified. The first, anomaly 24 near the Denali fault in the Slana River-Gillett Pass area, is due to a small ultramafic body. The other two, anomaly 25 in the extreme southeastern corner of the quadrangle and anomaly 26 just south of the headwaters of the Slana River, are due to Cretaceous (?) granitic intrusive rocks. Though its source rocks do not crop out, the magnetic high just east of Eagle Creek probably reflects a similar intrusion there (anomaly 27).

In addition to these relatively strong magnetic highs, reflecting intrusions with dimensions up to a few tens of km, the region east of the Chisna River lineament contains a number of low-amplitude magnetic highs observed on only one flight line. Such local magnetic highs, particularly where occurring over

mapped carbonate rocks, might indicate possible skarn deposits. The line spacing for this survey is too coarse to define all such bodies which may be present in this region. Additional close-spaced aeromagnetic and electromagnetic survey grids might be flown in order to isolate specific targets.

MAGNETIC MODELS

Figures 10 through 12 show models of magnetic structures along Profiles A-A', B-B', and C-C' (see Plate 2 for locations). These figures were made using a program by Campbell (1983).

The lower portion of each figure has a section view showing the assumed magnetic structures, whereas the upper portion has a plot showing observed magnetic field (solid curve) and calculated magnetic field (x's) which results from these structures. The section view (lower portion) has no vertical exaggeration. The fields are calculated on a datum (dashed line) which drapes topography at 0.3048 km, the nominal position of the survey aircraft. All bodies are presumed to be magnetized in the direction of the Earth's present-day field, of 57,000 nT magnitude, 76° inclination, and 28° easterly declination. The effective magnetic susceptibility used for each body is listed in Table 3, and is indicated by darker shading for higher susceptibilities. Unshaded portions of the section represent non-magnetic (very low susceptibility) rocks. For several bodies, particularly the Nikolai Greenstone and ultramafic rocks, the effective magnetic susceptibility includes an induced ("true" susceptibility) component, and an additional viscous natural remanent magnetization (NRM) component which is parallel to the Earth's present field and of magnitude comparable to the true component.

To do the calculations, the bodies shown were assumed to extend unchanged perpendicular to the plane of the section for varying strike-length distances Y1 and Y2 (Table 3), and then to be vertically cut off (the "2 1/2-dimensional geometry" of Shuey and Pasquale, 1973). The strike-lengths were chosen to match strike extents of corresponding anomalies on the aeromagnetic map. Contacts shown on these sections are thought to be correct to ±20°, at least near the surface. Errors in attitude modeling can be caused by using wrong strike-lengths, by differences in shape from the idealized prism supposed by the program, by non-uniform susceptibilities of source bodies, and by survey aircraft not being in the assumed position. Details of the bodies at depth are not well-controlled by the modeling process, and their bottoms could well be half as deep or twice as deep as is shown.

The geophysicist faces a fundamental ambiguity in modeling gravity and magnetic anomalies, for a certain anomaly may be caused by a deep-rooted, steep-sided body; by a shallow, thin

body with feather edges; or by any of a family of bodies between these two extremes (see Johnson and van Klinken, 1979, for examples.) The problem is particularly acute in handling broad, pervasive anomalies, which are presumably the most significant. Additional constraints are needed, preferably from seismic or electrical soundings, from drillholes, or from geologic mapping. Failing these, the geophysicist must rely on experience and intuition.

Table 3.--Parameters for interpreted bodies shown in figs. 10-12. Y1 and Y2 are distances the bodies are assumed to extend in front of and behind the plane of the figure, respectively.

Profile	Body	Y1 (km)	Y2 (km)	Susc. (S.I. x 10^{-5})	Represents
A-A'	1	1	10	7540	Ultramafic units
--	2	3	1	5026	Ultramafic units
--	3a	8	0.5	1508	Dike
--	3b	8	0.5	1885	Dike
--	4a	25	5	5026	Gakona Glacier body
--	4b	25	5	8796	Gakona Glacier body
B-B'	1	25	10	2386	Tangle Lakes pluton
--	2	10	30	8796	Amphitheatre ultramafic
--	3	0.3	12	4398	Nikolai Greenstone
--	4	0.3	0.3	4398	Nikolai Greenstone
--	5	12	15	1885	Slana subterrane
--	6	10	6	6283	Broxson Gulch body
--	7	6	6	628	Intrusive body
C-C'	1	10	40	729	Macomb intrusion
--	2	10	10	2764	Lake George body
--	3	10	10	2011	Lake George body
--	4	40	20	276	Lake George schists

Profile A-A'

Figure 10 shows models of possible magnetic structures along Profile A-A', which trends magnetic north (N28°E) across the Gakona Glacier body and Denali fault (location indicated on Plate 2). These figures have been discussed previously in a short article by Campbell and Nokleberg (1985). In that article, they show that if the Gakona Glacier body is assumed to be roughly equidimensional in cross-section, and if the Denali fault is assumed vertical in attitude, then there should be a substantial magnetic polarity low just north of the Denali fault. In fact, no such polarity low is observed. Errors in magnetic modeling can be caused by using wrong strike-lengths, by being too near the (assumed) vertically-truncated ends of the bodies being modeled, by strong remanent magnetism of source bodies, or by survey aircraft not being in the assumed position. All these

possibilities were examined, but none appears to explain the discrepancy.

All modeling here assumes rocks of the Jarvis Creek Glacier terrane and of the Windy terrane to be non-magnetic. This approximation seems to be fairly well justified. Except for a few samples from small mineral deposits located far from Profile A-A', all rock samples measured from these two terranes had susceptibilities below the threshold of our field susceptibility meter (0.0001 cgs units). Test models (not shown) indicate that if rocks of the Jarvis Creek Glacier subterrane are uniformly magnetized, their susceptibility must be less than 0.0005 cgs--above this level unmistakable magnetic highs would be seen over ridges. (There would still be a polarity low north of the (vertical) Denali fault, however.)

Figure 10 shows two interpretations that fit the observed magnetic fields: the lower section view, labeled (b) on figure 10, in which the Gakona Glacier body extends to very great depths (40 km, in the example shown) and has steep boundaries, and the upper section view, labeled (a), in which the body's bottom is constrained to more shallow depths, but its boundaries in turn must flare out at low angles. Both interpretations match observed magnetic fields equally well, but geologically they are very different. This example shows how dangerous it can be to accept any particular magnetic model without first investigating the range of permissible source bodies. In this case, interpretations (a) and (b) represent approximate end members of a series of intermediate interpretations which would also fit the observed magnetic field.

Interpretation (a) implies the Gakona Glacier body, and possibly the Denali fault as well, extends into the lower crust. Some geologists (e.g., Hamilton and Myers, 1967) believe typical batholiths are thin with respect to their widths, and so might prefer interpretation (b). In this instance, however, interpretation (b) requires either that the Denali fault dips at a rather shallow angle to the north, that the Gakona Glacier body was intruded after cessation of movement on the Denali fault, or that there is a magnetic body buried in the Jarvis Creek Glacier subterrane that just happens to be juxtaposed against the Denali fault at this place. Geologic mapping in this area (Nokleberg and others, 1982) shows that near the surface the Denali fault is approximately vertical. Forbes and others (1974) have shown that the Denali fault has a right lateral displacement since Cretaceous of 400 km. The recent-intrusion hypothesis is unlikely because Holocene igneous activity is unknown in this part of Alaska, and because the Denali fault appears from geologic and seismic evidence to be still active (Page, 1971; Lanphere, 1978). Further, the Denali fault appears from the aeromagnetic data to trim the northern edge of this particular

batholith for a distance of at least 40 km.

Might there be another magnetic body at depth, to the north of and juxtaposed directly against the Denali fault? Small magnetic bodies do occur elsewhere in the Jarvis Creek Glacier terrane, but there is no geologic evidence for a larger, buried one in this position. Such a body would have to have a special shape in order to so exactly cancel the expected polarity low there. In our earlier paper (Campbell and Nokleberg, 1985), therefore, we concluded that the Gakona Glacier body probably has a shape more like interpretation (a) than like interpretation (b). This conclusion indicated that at least one pluton in the study area is deep-rooted. Subsequent geophysical work, however, somewhat undermines our belief that a buried magnetic body is unlikely. Brocher and others (1991) report that a seismic profile that crossed the Denali fault along the Richardson Highway (very near A-A', that is) did not detect any particular contrast in seismic velocity between rocks on either side of the fault, although rocks of the Jarvis Creek Glacier subterrane were were much more anisotropic than those of the Slana River subterrane. Shallow seismic velocities increase from 3.5-3.7 km/s to 4.0-4.5 km/s north of the vicinity of the McCallum Creek/Slate Creek faults (the southern edge of the Gakona Glacier body?), but not at the Denali fault. Between the surface and 1 km depth, however, there is a northward-thinning wedge of 3.7-4.2 km/s material extending about 4 km north from the vicinity of the Denali fault.

Stanley and others (1990) report on three MT profiles crossing the Denali fault, one of which approximately follows A-A'. On the other two profiles the electrical conductivity at depths of about 2-15 km greatly increases immediately north of the Denali fault, but at A-A' it stays low for several km further to the north before the high electrical conductivities are seen that appear to be typical of the Yukon-Tanana terrane. This high conductivity zone, however, has no particular counterpart in the seismic interpretation, while the northward-thinning wedge interpreted from the seismic data is too shallow to be seen by MT. Nevertheless, both seismic and MT observations seem to be permissive of a buried intrusive body at depth in this area.

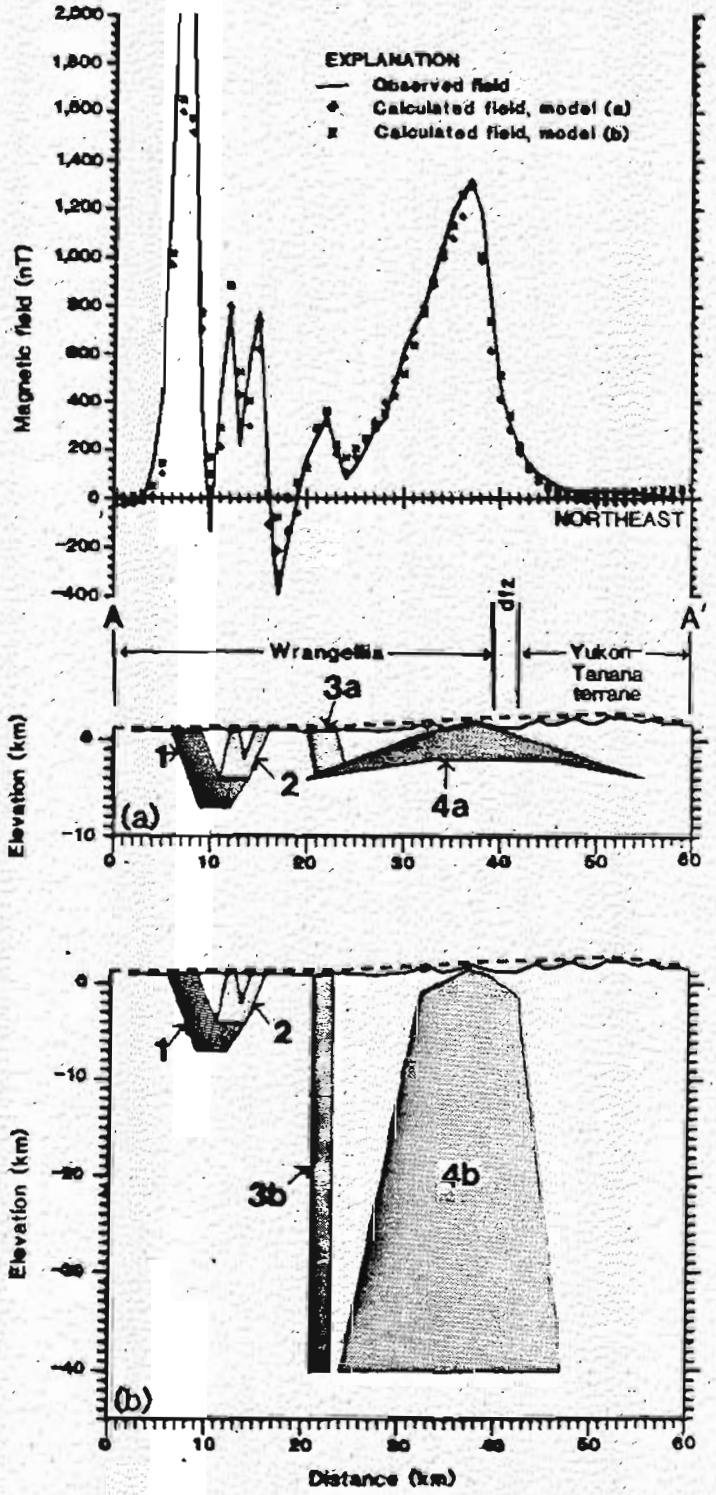

Figure 10.--Magnetic models of profile A-A' showing that good fits to the observed magnetic field can be made if it is assumed that (a) the Denali fault (df) dips to the north at a shallow angle or (b) the Gakona Glacier body (body 4) extends to great depths. Parameters for the bodies are listed in table 3. The surface location of the Denali fault is in the interval marked "dfz".

Profile B-B'

Figure 11 shows a model of magnetic structures along Profile B-B' made along flight line C-41 of the aeromagnetic map of the Mount Hayes quadrangle (State of Alaska, 1974). This model was discussed by Campbell and Nokleberg (1984). Its general features are similar to features on a cross section by Nokleberg and others (1981b), which was based solely on geologic mapping. Several features stand out. First is the thick high-susceptibility unit (body 3) making up part of the Amphitheatre Syncline. The unit is known to be cumulate mafic and ultramafic rock from occur in sparse outcrops along its northern flank. Plate 1 suggests body 3 is more extensive than was indicated by geologic mapping alone. Bodies 4 and 5 represent Nikolai Greenstone that crops out at that place on the profile. Their flat-laying attitude mirrors the disconformity which is known to exist between Nikolai Greenstone and underlying rocks. Bodies 1 and 2 lie south of the Paxson Lake fault and represent possible intrusive bodies of the northern part of the metamorphic complex of Gulkana River. Body 1 was modeled and discussed by Campbell and Nokleberg (1986) on a southern extension of profile B-B'.

The position of the Eureka Creek thrust shown on the figure is not precisely controlled geologically at the place where it cuts the section. Assuming that the Eureka Creek thrust forms the southern boundary of body 6, figure 11 suggests that its true position may be 1-2 km to the south of the marked location. Body 6 then would represent most or all of the Slana River subterrane, a moderately magnetic sliver of island-arc volcanic and sedimentary rocks. Its sole is here taken to be 10 km below sea level, but this depth is not well controlled.

The Broxson Gulch thrust appears in this model to be dipping about 30° to the north, and to be floored by a high-susceptibility sheet (body 7). This sheet lies entirely within the Slana River subterrane, and at the profile occurs just south of the thrust. Just a few km east of this profile, however, the sheet migrates south into the Slana River subterrane, away from the mapped position of the thrust. Body 7 may represent one of several fault-bounded units of cumulative mafic and ultramafic rock in this vicinity which dip moderately north (Nokleberg and others, 1982). Body 8 is a weakly-magnetized zone which straddles an unnamed fault separating the Windy terrane from the Aurora Peak terrane. The shape and structure of this body or complex of bodies cannot be found magnetically due to its low susceptibility. In particular, its northern and southern edges (possibly representing splays of the Denali fault) may be substantially changed but still provide a good fit to the observed magnetic field.

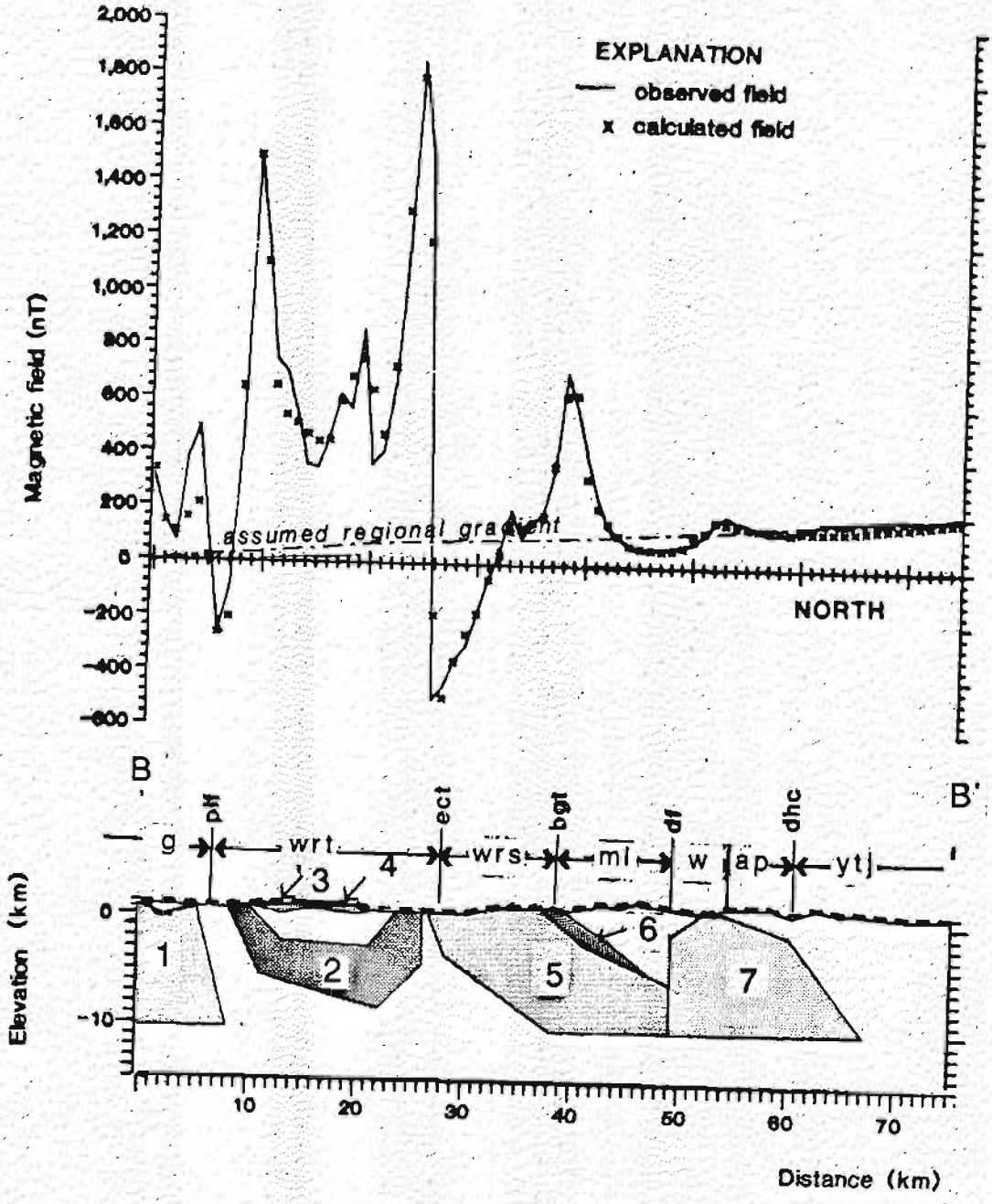

Figure 11.--Magnetic model of Profile B-B' extending northward from the southern edge of the Mount Hayes quadrangle along meridian 146°00'. Major faults crossed are the Paxon Lake fault (plf), Eureka Creek fault (ect), Broxson Gulch thrust (bgt), Denali fault (df) and Hines Creek fault (dhc). Terrane abbreviations from figure 2. Bodies modeled here include (1) a pluton near Tangle Lakes, (2) a thick, concave-upward ultramafic sill (heavy shading) in a lower portion of the Amphitheatre Syncline, (3) and (4) units of Nikolai Greenstone, (5) a moderately-magnetic unit of the Slana River subterrane (light shading) bounded on the south by the Eureka Creek fault, (6) a thin, planar, very-magnetic unit (heavy shading) which parallels the Broxson Gulch thrust, and (7) a pluton whose southern edge may have been truncated by the Denali fault. Parameters for the bodies are listed in table 3.

Profile C-C'

Figure 12 shows a model of magnetic structures along Profile C-C' made along flight line D-95 of the aeromagnetic map of the Mount Hayes quadrangle (State of Alaska, 1974). The higher-susceptibility Lake George body and lower-susceptibility body of the Macomb subterrane are shown. Following the convention used in making the models in both figures 11 and 12, the bottoms of these bodies have been placed at a depth of 10 km below sea level. As indicated in the discussion near table 3, however, true depth-extents of these modeled bodies may differ from this assumed value.

This profile was modeled to try to estimate the nature and depth-configurations of the Sand Creek lineament (Plate 2) and the Tanana River fault. Such magnetic features are best modeled using profiles that cross them at right angles. Profile C-C', however, crosses these two features at substantial, though opposite, angles; the modeling, therefore, is even more approximate than usual. Still, it appears that most or all of the Sand Creek lineament reflects the northwest edge of outcrops or subcrops of a granitic body (body 1) that intruded into the Macomb and Lake George subterranes. Subsurface parts of the intrusion may extend substantially further to the northwest. The Sand Creek lineament does not seem to be offset by the Tanana River fault, unless rocks with similar magnetic properties occur on both sides. The model suggests that the Tanana River fault (boundary(?) between bodies 1 and 2) may dip to the north and northeast. The model also suggests that source rocks for the Lake George magnetic high (bodies 2 and 3) have differing susceptibilities, perhaps indicating a composite intrusion there. Finally, rocks of the Lake George subterrane which resist erosion well enough to make ridges, like those forming ridges in other subterranes of the Yukon-Tanana terrane, are mildly magnetic and will give rise to subtle magnetic highs over ridges (body 4).

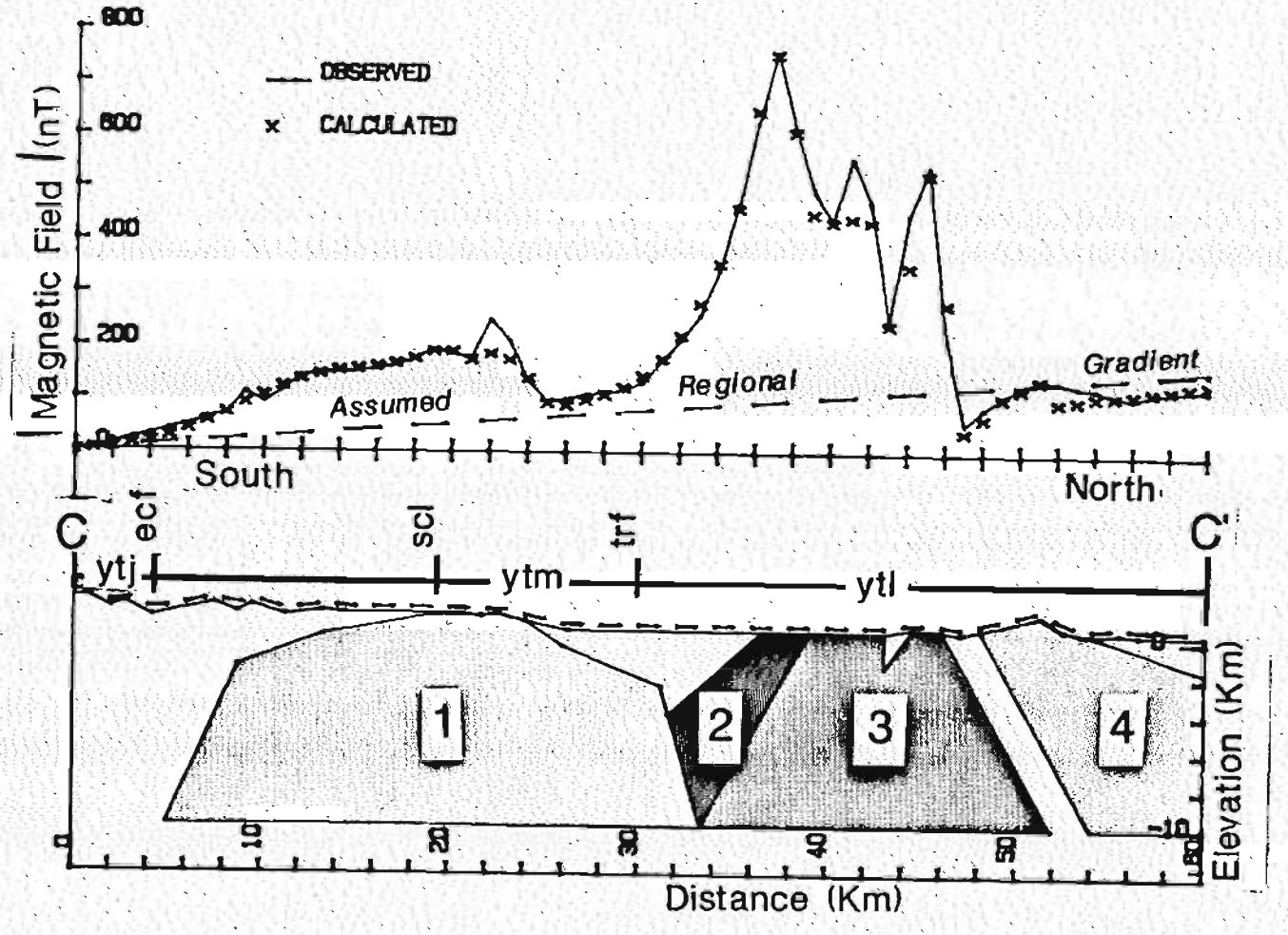

Figure 12.--Magnetic model of Profile C-C' extending southward from the northern edge of the Mount Hayes quadrangle along flight line P-95. Faults and lineaments crossed are the Elting Creek fault (ecf), Sand Creek lineament (scl), and Tanana River fault (trf). Magnetic bodies modeled here include: (1) the Macomb intrusive body, (2) a particularly magnetic unit south of the Lake George pluton, (3) the Lake George pluton, and (4) a mildly magnetic unit representing rocks that form ridges in the subterrane. Parameters for the bodies are listed in table 3. ytj, Jarvis Creek Glacier subterrane of Yukon-Tanana terrane; ytm, Macomb subterrane of Yukon-Tanana terrane; ytl, Lake George subterrane of Yukon-Tanana terrane.

REFERENCES CITED

Aleinikoff, J.N., and Nokleberg, W.J., 1985, Age of Devonian igneous-arc terranes in the northern Mount Hayes quadrangle, eastern Alaska Range, Alaska, in Bartsch-Winkler, S., ed., The United States Geological Survey in Alaska -- Accomplishments during 1984: U.S. Geological Survey Circular 967, p. 44-49.

Andreasen, G.E., Grantz, Arthur, Zietz, Isidore, and Barnes, D.F., 1964, Geologic interpretation of magnetic and gravity data in the Copper River Basin, Alaska: U.S. Geological Survey Professional Paper 316-H, p. 135-153, and 2 plates.

Barnes, D.F., Mariano, John, Morin, R.L., Roberts, C.W., and Jachens, R.C., 1994, Incomplete isostatic gravity map of Alaska, Plate 9, *in* Plafker, George, and Berg, H.C., *eds.*, The Geology Of Alaska, DNAG volume G-1: Boulder CO: Geological Society of America, scale 1:2,500,000.

Barnes, D.F., Nokleberg, W.J., and Brocher, T.M., 1991, Gravitational and seismic evidence for Tertiary structural basins in the Alaska Range and Tanana lowland (abs.): Geological Society of America Abstracts with Programs, v. 23, no. 2, p.5.

Brocher, T.M., Nokleberg, W.J., Christensen, N.I., Lutter, W.J., Geist, E.L., and Fisher, M.A., 1991, Seismic reflection/refraction mapping of the faulting and regional dips in the eastern Alaska Range: Journal of Geophysical Research, v. 96, p. 10,233-10,249.

Bond, G.C., 1976, Geology of the Rainbow Mountain-Gulkana Glacier area, eastern Alaska Range, with emphasis on upper Paleozoic strata: Alaska Division of Geological and Geophysical Surveys Geological Report 45, 47 p.

Campbell, D.L., 1983, BASIC programs to calculate gravity and magnetic anomalies due to 2 1/2-dimensional prismatic bodies: U.S. Geological Survey Open-File Report 83-154, 38 p.

Campbell, D.L., 1986, Profiles showing models of magnetic structures in accreted terranes of south-central Alaska: U.S. Geological Survey Miscellaneous Field Studies Map MF-1912, 2 sheets, scale 1:500,000.

Campbell, D.L., 1989, Gravity and magnetic models of profiles near Richardson Highway, southern Alaska, *in* Nokleberg, W.J., and Fisher, M.A., *eds.*, Alaskan geological and geophysical transect: 27th International Geological Congress, Guidebook T104, p. 69-74.

Campbell, D.L., and Nokleberg, W.J., 1984, Magnetic profile across accreted terranes, Mount Hayes quadrangle, eastern Alaska Range, Alaska in Bartsch-Winkler, S., and Reed, K., eds., U.S. Geological Survey in Alaska--Accomplishments during 1982: U.S. Geological Survey Circular 939, p. 44-47.

Campbell, D.L., and Nokleberg, W.J., 1985, Magnetic profile across Denali fault, Mount Hayes quadrangle, eastern Alaska Range, Alaska in Bartsch-Winkler, S., ed., U.S. Geological Survey in Alaska--Accomplishments during 1983: U.S. Geological Survey Circular 945, p. 68-72.

Campbell, D.L., and Nokleberg, W.J., 1986, Magnetic model of a profile across the northern Copper River basin, northeastern Gulkana quadrangle in Bartsch-Winkler, S., and Reed, K.M., eds., Geological Studies in Alaska by U.S. Geological Survey during 1985: U.S. Geological Survey Circular 978, p. 35-38.

Case, J.E., and MacKevett, E.M., Jr., 1976, Geologic interpretation of aeromagnetic map, McCarthy quadrangle, Alaska: U.S. Geological Survey Miscellaneous Field Studies Map MF-773-D, 2 sheets, scale 1:250,000.

Cunningham, C.G., Steven, T.A., Campbell, D.L., Naeser, C.W., Pitkin, J.A., and Duval, J.S., 1984, Multiple episodes of igneous activity, mineralization, and alteration in the western Tushar Mountains: U.S. Geological Survey Bulletin 1299-A, 21 p.

Curtin, G.C., Tripp, R.C., and Nokleberg, W.J., 1989, Summary and interpretation of geochemical maps for stream sediment and heavy mineral concentrate samples, Mount Hayes quadrangle, eastern Alaska Range, Alaska: U.S. Geological Survey Miscellaneous Field Investigations Map MF-1996-B, 3 sheets (scale 1:250,000) and 11 pages.

Forbes, R.B., Smith, T.E., and Turner, D.L., 1974, Comparative petrology and structure of the Maclaren, Ruby Range, and Coast Range belts--implications for offset along the Denali fault system: Geological Society of America Abstracts with Programs, v. 6, p. 177.

Grauch, V.J.S., and Campbell, D.L., 1983, Does draping aeromagnetic surveys reduce terrain-induced effects?: Geophysics v. 49, p. 75-80.

Griscom, Andrew, 1977, Aeromagnetic map and interpretation of the Tanacross quadrangle, Alaska: U.S. Geological Survey Miscellaneous Field Studies Map MF-767A, 2 sheets, scale 1:250,000.

Hamilton, Warren, and Myers, W.B., 1967, The nature of batholiths: U.S. Geological Survey Professional paper 554-C, 30 p.

Hillhouse, J.W., and Gromme, C.S., 1984, Northward displacement and accretion of Wrangellia--new paleomagnetic evidence from Alaska: Journal of Geophysical Research, v. 89, no. B6, p. 4461-4477.

Hoover, D.B., Heran, W.D., and Hill, P.L., 1992, The geophysical expression of selected mineral deposit models: U.S. Geological Survey Open-File Report 92-557, 129 p.

Johnson, B.D., and van Klinken, Gerry, 1979, Some equivalent bodies and ambiguity in magnetic and gravity interpretation: Bulletin Australian Society of Exploration Geophysicists, v. 10, no. 1, p. 109-110.

Jones, D.L., Silberling, N.J., Berg, H.C., and Plafker, George, 1981, Map showing tectonostratigraphic terranes of Alaska, columnar sections, and summary description of terranes: U.S. Geological Survey Open-File Report 81-793, 20 p. plus 2 plates.

Labson, V.F., and Stanley, W.D., 1989, Electrical resistivity structure beneath southern Alaska: in Nokleberg, W.J., and Fisher, M.A., eds, Alaskan Geological and Geophysical Transect, Valdez to Coldfoot, Alaska: American Geophysical Society Field Trip Guidebook T104, p. 75-78.

Lanphere, M.A., 1978, Displacement history of the Denali fault system, Alaska

and Canada: Canadian Journal of Earth Sciences, v. 15, p. 817-822.

Matteson, Charles, 1973, Geology of the Slate Creek area, Mount Hayes A-2 quadrangle, Alaska [M.S. thesis]: Fairbanks, University of Alaska, 66 p.

MacKevett, E.M., Jr., 1978, Geologic map of McCarthy quadrangle, Alaska: U.S. Geological Survey Miscellaneous Investigations Map MI-1032, 1 sheet, scale 1:250,000.

Meyer, John F., Jr., and Saltus, R.W., 1995, Merged aeromagnetic map of interior Alaska: U.S. Geological Survey Geophysical Map GP-1014, 4 sheets, scale 1:500,000.

Meyer, John F., Jr., Saltus, R.W., Barnes, D.F., and Morin, R.L., 1996, Bouguer gravity map of interior Alaska, U.S. Geological Survey Geophysical Map GP-1016, 2 sheets, scale 1:500,000.

Nokleberg, W.J., Albert, N.D.R., Bond, G.C., Herzon, P.L., Miyaoka, R.T., Nelson, W.H., Richter, D.R., Smith, T.E., Stout, J.H., Yeend, W., and Zehner, R.E., 1982, Geologic map of the southern part of the Mount Hayes quadrangle, Alaska: U.S. Geological Survey Open-File Report 82-52, 1 sheet, scale 1:250,000, 26 p.

Nokleberg, W.J., Albert, N.R.D., Herzon, P.L., Miyaoka, R.T., and Zehner, R.E., 1981a, Recognition of two subterranes within the Wrangellia terrane, southern Mount Hayes quadrangle, Alaska in Albert, N.R.D., and Hudson, Travis, eds., the United States Geological Survey in Alaska--Accomplishments during 1979: U.S. Geological Survey Circular 823-B, p. B64-B66.

Nokleberg, W.J., Albert, N.R.D., Herzon, P.L., Miyaoka, R.T., and Zehner, R.E., 1981b, Cross section showing accreted Andean-type arc and island arc terranes in southwestern Mount Hayes quadrangle, Alaska in Albert, N.R.D., and Hudson, Travis, eds., the United States Geological Survey in Alaska -- Accomplishments during 1979: U.S. Geological Survey Circular 823-B, p. B66-B67.

Nokleberg, W.J., and Aleinikoff, J.N., 1985, Summary of stratigraphy, structure, and metamorphism of Devonian igneous-arc terranes, northeastern Mount Hayes quadrangle, eastern Alaska Range in Bartsch-Winkler, S., ed., The United States Geological Survey in Alaska--Accomplishments during 1984: U.S. Geological Survey Circular 967, p. 66-71.

Nokleberg, W.J., Aleinikoff, J.N., Dutro, J.T., Jr., Lanphere, M.A., Silberling, N.J., Silva, S.R., Smith, T.E., and Turner, D.L., 1992, Map, tables, and summary of fossil and isotopic age data, Mount Hayes quadrangle, eastern Alaska Range, Alaska: U.S. Geological Survey Miscellaneous Field Studies Map MF-1996-D, 1 sheet (scale 1:250,000) and 43 p.

Nokleberg, W.J., Aleinikoff, J.N., Lange, I.M., Silva, S.R., Miyaoka, R.T., Schwab, C.E., and Zehner, R.E., with contributions for selected areas from Bond, G.C., Richter, D.H., Smith, T.E., and Stout, J.H., 1992, Preliminary geologic map of the Mount Hayes quadrangle, eastern Alaska Range, Alaska: U.S. Geological Survey Open-file Report 92-594, 1 sheet (scale 1:250,000) and 39 p.

Nokleberg, W.J., Jones, D.L., and Silberling, N.J., 1985, Origin and tectonic evolution of the Maclaren and Wrangellia terranes, eastern Alaska Range, Alaska: Geological Society of America Bulletin, v. 96, p. 1251-1270.

Nokleberg, W.J., Lange, I.M., Roback, R.C., Yeend, Warren, and Silva, S.R., 1991, Map showing locations of metalliferous lode and placer mineral occurances, prospects, and mines, Mount Hayes quadrangle, eastern Alaska Range, Alaska: U.S. Geological Survey Miscellaneous Field Studies Map MF-1996-C, 42 p., 1 sheet, scale 1:250,000.

Nokleberg, W.J., Lange, I.M., Singer, D.A., Curtin, G.C., Tripp, R.B., Campbell, D.L., and Yeend, Warren, 1990, Metalliferous mineral resource assessment maps of the Mount Hayes quadrangle, eastern Alaska Range, Alaska: U.S. Geological Survey Miscellaneous Field Studies Map MF-1996-1, 4 sheets, scale 1:250,000.

Nokleberg, W.J., Plafker, George, and Wilson, F.H., 1994, Geology of south-central Alaska, *in* Plafker, George, and Berg, H.C., *eds.*, The Geology of Alaska, DNAG volume G-1: Boulder CO: Geological Society of America, Chapter 10, pps. 311-366.

Nokleberg, W.J., Wade, W.M., Lange, I.M., and Plafker, George, 1986, Summary of geology of the Peninsular terrane, metamorphic complex of Gulkana River, and Wrangellia terrane, north-central andnorthwestern Gulkana quadrangle in Bartsch-Winkler, Susan, and Reed, K.M., eds., Geological studies in Alaska by U.S. Geological Survey during 1985: U.S. Geological Survey Circular 978, p. 69-73.

Page, R.A., 1971, Microearthquakes of the Denali fault near the Richardson Highway, Alaska: EOS (Amer. Geophys. Union Trans.), v. 52, p. 278.

Plafker, G., Nokleberg, W.J., and Lull, J.S., 1989, Bedrock geology and tectonic evolution of the Wrangellia, Peninsular, and Chugach terranes along the Trans-Alaskan Crustal Transect in the northern Chugach Mountains and southern Copper River basin, Alaska: Journal of Geophysical Research, v. 94, p. 4255-4295.

Portnov, A.M., 1987, Specialization of rocks toward potassium and thorium in relation to mineralization: International Geology Review, v. 29, p. 326-344.

Reid, A.B., 1980, Aeromagnetic survey design: Geophysics, v. 45, p. 973-976.

Richter, D.H., and Dutro, J.T., Jr., 1975, Revision of type Mankomen Formation (Pennsylvanian and Permian), Eagle Creek area, eastern Alaska Range, Alaska: U.S. Geological Survey Bulletin 1395-B, 25 p.

Richter, D.H., Lanphere, M.A., and Matson, N.A., 1975, Granitic plutonism and metamorphism, eastern Alaska Range, Alaska: Geol. Society of America Bulletin, v. 86, p. 819-829.

Richter, D.H., Sharp, W.N., Dutro, J.T., Jr., and Hamilton, W.B., 1977, Geologic map of parts of the Mount Hayes A-1 and A-2 quadrangles, Alaska: U.S. Geological Survey Miscellaneous Investigations Series Map I-1031, 1 sheet, scale 1:63,360.

Rose, A.W., 1965, Geology and mineral deposits of the Rainy Creek area, Mount Hayes quadrangle, Alaska: Alaska Division of Mines and Minerals

Geologic Report 14, 51 p.

Rose, A.W., 1966a, Geology of part of the Amphitheater Mountains, Mount Hayes quadrangle, Alaska: Alaska Division of Mines and Minerals Geologic Report 19, 14 p.

Rose, A.W., 1966b, Geological and geochemical investigations in the Eureka Creek and Rainy Creek areas, Mount Hayes quadrangle, Alaska: Alaska Division of Mines and Minerals Geologic Report 20, 36 p. 32

Rose, A.W., 1967, Geology of the Chistochina River area, Mount Hayes quadrangle, Alaska: Alaska Division of Mines and Minerals Geologic Report 28, 39 p.

Rose, A.W., and Saunders, R.H., 1967, Geology and geochemical investigations near Paxson, northern Copper River Basin, Alaska: Alaska Division of Mines and Minerals Geologic Report 13, 35 p.

Saltus, R.W., Meyer, J.F., Jr., Barnes, D.F., and Morin, R.L., 1997, Tectono-geophysical domains of interior Alaska as interpreted from new gravity and aeromagnetic data compilations, in Dumoulin, J.A., and Gray, J.A., eds., Geological studies in Alaska by U.S. Geological Survey during 1995: U.S. Geological Survey Professional Paper 1574, p. 157-171.

Shuey, R.T., and Pasquale, A.S., 1973, End corrections in potential field modeling: Geophysics, v. 38, p. 507-512.

Simpson, R.W., Jachens, R.C., Blakely, R.J., and Saltus, R.W., 1986, A new isostatic residual gravity map of the conterminous United States with a discussion on the significance of isostatic residual anomalies: Journal of Geophysical Research, v. 91, p. 8348-8372.

Stanley, W.D., Labson, V.F., Nokleberg, W.J., Csejtey, Bela, Jr., and Fisher, M.A., 1990, The Denali fault system and Alaska Range of Alaska: Evidence for underplated Mesozoic flysch from magnetotellurics: Geol. Society of America Bulletin, v. 102, p. 160-173.

State of Alaska, 1974, Aeromagnetic Survey, East Alaska Range, Mount Hayes, Alaska: Division of Geological and Geophysical Surveys Map AOF-10, scale 1:250,000.

Stout, J.H., 1976, Geology of the Eureka Creek area, east-central Alaska Range, Alaska: Alaska Division of Geological and Geophysical Surveys Geologic Report 46, 32 p.

Texas Instruments, Inc., 1978, Aerial Radiometric and Magnetic Reconnaissance Survey of the Eagle-Dillingham Area, Alaska -- Mount Hayes Quadrangle, Volume 2-H: U.S. Energy Research and Development Administration, Grand Junction Office Report GJBX-113(78), scale 1:500,000.

U.S. Geological Survey, 1985, Composite aeromagnetic map of part of the Wrangell Mountains, Alaska: U.S. Geological Survey Open-File Report 85-605, 1 sheet, scale 1:250,000.

APPENDIX -- DESCRIPTION OF MAP UNITS (PLATE 2)

Qs **Surficial deposits (Quaternary)**—Alluvium, colluvial deposits, glacial deposits, fluviolacustrine deposits, rock-glacier deposits, snow, and ice

SEDIMENTARY ROCKS AND METAMORPHOSED SEDIMENTARY, VOLCANIC, AND PLUTONIC ROCKS (NORTH OF DENALI FAULT)

SEDIMENTARY AND IGNEOUS ROCKS (NORTH OF DENALI FAULT)

Tn **Nenana Gravel (late Tertiary)**—Chiefly thick-bedded to massive, poorly sorted conglomerate with lesser sandstone and siltstone. Unconformably overlain by Pleistocene glacial deposits. Locally unconformably overlies sandstone unit (Ts) of Oligocene to Pliocene age, and locally overlies coal-bearing sedimentary rocks of Jarvis Creek coal field of early Tertiary age

Ts **Sandstone (late and middle Tertiary)**—Chiefly sandstone, graywacke, poorly consolidated siltstone, and mudstone. Found mainly in fault-bounded prisms along northern extent of Alaska Range. Locally overlain by Nenana Gravel and locally overlies sedimentary rocks of Jarvis Creek coal field (Tsj). Unit age is Oligocene, Miocene, and Pliocene

Tsj **Sedimentary rocks of Jarvis Creek coal field (early Tertiary)**—Chiefly conglomerate, sandstone, and coal beds. Locally overlain by sandstone unit (Ts) and Nenana Gravel (Tn)

la **Lamprophyre, alkalic gabbro, and alkalic diorite (early Tertiary and Late Cretaceous)**—Chiefly fine- to medium-grained, panidiomorphic-granular aggregates of olivine, orthopyroxene, clinopyroxene, hornblende, biotite, plagioclase, and potassium-feldspar with varying amounts of groundmass. Groundmass consists of fine-grained hornblende, biotite, plagioclase, and opaques and interstitial or replacement carbonate. Local embayed phenocrysts. Found in locally abundant dikes and sills, local small plutons, and in igneous complex of Mount Hajdukovich in north-central part of quadrangle

md **Monzonite and diorite (early Tertiary and Late Cretaceous)**—Chiefly fine- to medium-grained, hypautomorphic-granular aggregates of clinopyroxene, biotite, potassium feldspar, and plagioclase. Local white mica and carbonate alteration. Found in moderate-size plutons in igneous complex of Mount Hajdukovich in north-central part of quadrangle

grn **Granitic plutonic rocks north of Denali fault (early Tertiary to Late Cretaceous)**—Chiefly medium- to coarse-grained biotite-hornblende granite and hornblende-biotite granodiorite with lesser quartz diorite and diorite. Predominate igneous rather than metamorphic textures. Present as small dikes, stocks, and locally large plutons in southern Yukon-Tanana, Aurora Peak, and Windy terranes. Locally weakly to moderately deformed and metamorphosed at lower greenschist facies in Macomb Plateau area. Local intense hydrothermal alteration

gb **Gabbro and mafic plutonic rocks and dikes and sills (Cretaceous)**—Chiefly gabbro and metagabbro with lesser hornblende diorite and diabase. Intrudes Jarvis Creek Glacier and Hayes Glacier subterranes (of southern Yukon-Tanana terrane) and Windy terrane. Textures in gabbro, diorite, and diabase mainly hypautomorphic-granular or ophitic aggregates of

hornblende, plagioclase and lesser biotite. Textures in metagabbro mainly schistose aggregates of actinolite, chlorite, biotite, epidote, and albite. Found in narrow dikes to small- to moderate-size plutons. Dikes and sills generally subconcordant to acutely crossing intense schistosity and parallel compositional layering in wall rocks. Crosscut and intruded by Cretaceous and early Tertiary granitic rocks

YUKON-TANANA TERRANE

Lake George subterrane
(North of Tanana River fault)

lga **Augen gneiss and schist (Mississippian)**—Coarse- to medium-grained augen gneiss and schist composed of gneissose aggregates of potassium feldspar, plagioclase, biotite, and quartz. Ductilely deformed and regionally metamorphosed at amphibolite facies into mylonitic gneiss and schist. Found in moderate- to large-size, irregularly shaped, homogeneous plutons intruding gneissose granitic plutons and pelitic schist. Relict hypautomorphic-granular texture with relict potassium feldspar phenocrysts. Locally deformed and retrograded to lower greenschist facies

lgr **Medium-grained gneissose granitic rocks (Devonian)**—Chiefly gneissose hornblende-biotite granodiorite and lesser gneissose biotite granite. Relict hypautomorphic-granular texture. Found in moderate- to large-size, irregularly shaped, homogeneous plutons intruding pelitic schist. Ductilely deformed and regionally metamorphosed at amphibolite facies into mylonitic gneiss. Locally deformed and retrograded to lower greenschist facies

lgs **Pelitic schist and quartzite (Devonian and older)**—Chiefly polydeformed, medium- to coarse-grained pelitic muscovite-quartz-biotite-garnet schist and metaquartzite derived from quartz-rich to clay-rich shale. Ductilely deformed and regionally metamorphosed at amphibolite facies into mylonitic schist. Locally deformed and retrograded to lower greenschist facies

Macomb subterrane
(South of Tanana River fault)

mg **Medium-grained granitic gneiss (Devonian)**—Chiefly fine- to medium-grained gneissose granite and granodiorite with lesser quartz diorite and diorite. Ductilely deformed and regionally metamorphosed into mylonitic gneiss at epidote-amphibolite facies. Form irregularly shaped plutons and dikes intruding pelitic schist, calc-schist, and quartz-feldspar schist. Locally deformed and retrograded to lower greenschist facies

ms **Metamorphosed pelitic, calcareous, and quartz-feldspar sedimentary rocks (Devonian or older)**—Medium-grained, polydeformed, biotite-muscovite-quartz pelitic schist, garnet-plagioclase schist, and quartz-plagioclase-biotite schist derived from shale, marl, and sandstone. Ductilely deformed and regionally metamorphosed at epidote-amphibolite facies

into fine- to medium-grained mylonitic schist. Locally deformed and retrograded to lower greenschist facies

Jarvis Creek Glacier subterrane
(South of Elting Creek fault)

jcg **Fine- to medium-grained gneissose granitic rocks (Devonian)**—Chiefly gneissose hornblende-biotite diorite and granodiorite and lesser augen gneiss or gneissose granite. Found in small- to moderate-size, irregularly shaped, homogeneous plutons. Relict hypautomorphic-granular texture. Mainly in Donnelly Dome and benchmark Ober areas intruding pelitic schist and quartzite. Ductilely deformed and regionally metamorphosed at amphibolite facies into mylonitic gneiss and schist. Local retrogression to south to lower greenschist facies

jcv **Fine-grained schistose metavolcanic and metasedimentary rocks (Devonian)**—Chiefly polydeformed, fine-grained, schistose meta-andesite and metamorphosed quartz keratophyre with lesser metadacite, metabasalt, pelitic schist, quartzite, calc- schist, and marble. Ductilely deformed and regionally metamorphosed at greenschist facies into mylonitic schist or local phyllonite. Local intense iron staining, and disseminated and massive sulfide minerals

jcs **Fine-grained metasedimentary rocks (Devonian and older)**—Chiefly polydeformed, fine-grained pelitic schist and quartzite with lesser calc-schist, quartz feldspar schist and marble, and with very sparse schistose metavolcanic rocks. Metasedimentary rocks derived from shale, chert or quartz sandstone, marl, volcanic graywacke, and limestone. Ductilely deformed and regionally metamorphosed at greenschist facies into mylonitic schist or local phyllonite. Includes large areas of upper greenschist facies and lower amphibolite facies metamorphic rocks in area south of Granite Mountain and south of Donnelly Dome. Amphibolite facies minerals to north are progressively replaced by greenschist-facies minerals to south

Hayes Glacier subterrane
(South of Hines Creek and Mount Gakona faults)

hgv **Fine-grained schistose volcanic rocks and phyllite (Devonian)**—Chiefly polydeformed, schistose to phyllitic meta-andesite and metamorphosed quartz keratophyre, and lesser metadacite and metabasalt with locally abundant pelitic-, quartz-, and calc-phyllite. Ductilely deformed and regionally metamorphosed at lower- and middle-greenschist facies into phyllonite and blastomylonite. Local areas of iron staining and disseminated sulfide minerals

hgs **Fine-grained schistose sedimentary rocks and volcanic rocks (Devonian and older)**—Chiefly pelitic, quartz-, and calc-phyllite. In eastern part of quadrangle, chiefly polydeformed quartz-chlorite-white mica phyllite, graphitic-quartz phyllite, quartz-plagioclase phyllite, calc-phyllite, and marble. Locally meta-andesite, metamorphosed quartz keratophyre, and metadacite. In western part of quadrangle, chiefly polydeformed pelitic schist, quartz-mica schist, and lesser quartzite, and calc-schist derived from shale, quartz-siltstone and sandstone, and marble. Derived from shale, chert or quartz siltstone, volcanic graywacke, marl, and limestone. Ductilely deformed and regionally metamorphosed at lower and middle greenschist facies into phyllonite and blastomylonite

AURORA PEAK TERRANE
(SOUTH OF NENANA GLACIER FAULT AND NORTH OF DENALI FAULT)

ag **Metamorphosed granitic rocks (Late to mid-Cretaceous)**—Chiefly gneissose granodiorite and granite with lesser quartz diorite, diorite, gabbro, and amphibolite derived from gabbro and diorite. Found in east-striking plutons and dikes intruding calc-schist, marble, quartzite, and pelitic schist. Relict hypautomorphic granular texture. Ductilely metamorphosed and penetratively deformed twice, once into mylonitic gneiss during earlier period of upper amphibolite facies metamorphism, and later into blastomylonite during period of middle greenschist-facies metamorphism

as **Metamorphosed sedimentary rocks (Triassic to Silurian)**—Chiefly polydeformed, fine- to medium-grained calc-schist, marble, quartzite, and pelitic schist. Derived from marl, quartzite, and shale. Ductilely metamorphosed and deformed twice, once into mylonitic schist during older period of upper amphibolite facies metamorphism and later into blastomylonite at middle-greenschist facies

WINDY TERRANE
(WITHIN SPLAYS OF DENALI FAULT)

wm **Melange (Cretaceous, Devonian, and Silurian?)**—Structural melange consisting of two assemblages: (1) small to large fault-bounded lenses of Cretaceous flysch and volcanic rocks, mainly argillite, quartz-pebble siltstone, quartz sandstone, metagraywacke, and conglomerate with lesser andesite and dacite; and (2) small to large fault-bounded lenses of limestone and marl of Silurian(?) and Devonian age. Weakly metamorphosed. Local weak schistosity. Locally intensely deformed locally, with development of phyllonite and protomylonite in narrow shear zones. Incipient lower greenschist-facies metamorphism. Found as in narrow, fault-bounded lenses along Denali fault

SEDIMENTARY AND VOLCANIC ROCKS AND
METAMORPHOSED SEDIMENTARY, VOLCANIC, AND PLUTONIC ROCKS
(SOUTH OF DENALI FAULT)

Tsc **Sandstone and conglomerate (late to early Tertiary)**—Chiefly continental clastic deposits of light-colored, fine-grained, poorly sorted, sandstone with locally interbedded siltstone, pebbly sandstone, pebble to cobble conglomerate, and sparse thin coal layers, and sparse white rhyodacite ash layers south of The Hoodoos. Found in scattered exposures. Overlies the conglomerate unit (Tc). Generally faulted against older bedrock. Commonly found as fault-bounded lenses in branches of Broxson Gulch thrust, Rainy Creek thrust, and Eureka Creek fault. Unit age is considered to be Eocene to Miocene

Tc **Conglomerate (early Tertiary)**—Chiefly continental clastic deposits of mainly poorly sorted, crudely bedded to massive, polymictic conglomerate and lesser sandstone. Conglomerate contains abundant clasts of rhyodacite to dacite tuff and flows, Nikolai Greenstone, argillite, volcanic sandstone, and andesite to dacite flows of Eagle Creek and Slana Spur Formations, quartz diorite, greenschist, gabbro, and ultramafic rocks. Local thin beds of coal in sandstone layers. Overlies volcanic rocks unit (Tv) and older bedrock of Slana Spur Formation. Locally faulted against older bedrock. Commonly found as fault-bounded

lenses in branches of McCallum Creek-Slate Creek thrust. Unit age is considered to be Eocene

Tv **Volcanic rocks (early Tertiary)**—Chiefly ash-flow tuff, breccia, agglomerate, flows, dikes, and sills with lesser volcanic sandstone, conglomerate, and limestone, dikes, and sills. Igneous rocks chiefly rhyodacite, dacite, and andesite. Found as scattered outcrops. Overlain by, and locally in fault contact with conglomerate unit (Tc) and sandstone and conglomerate unit (Tsc). Locally faulted against older bedrock of Slana Spur Formation. Unit age is considered to be Eocene

grs **Granitic plutonic rocks south of Denali fault (early tertiary Cretaceous, and Late Jurassic)**—Chiefly medium- to coarse-grained hornblende-biotite granodiorite and biotite granite with lesser diorite and quartz diorite. Predominant texture igneous rather than metamorphic. Found in Maclaren, Clearwater, and Wrangellia terranes in small dikes, stocks, and moderate-size to large plutons. Weakly deformed to nonschistose. Locally weakly to extensively hydrothermally altered

TERRANE OF ULTRAMAFIC AND ASSOCIATED ROCKS

um **Ultramafic and associated rocks (Mesozoic?)**—Partly serpentinized. Includes lesser hornblende-plagioclase gneiss, and minor serpentinite, marble, graphitic schist, tonalite, and granite. Earlier pervasive ductile deformation and metamorphism at amphibolite facies. Locally well defined schistosity. Later, locally,intensely deformed and metamorphosed to lower greenschist. Found as narrow, fault-bounded lens along Denali fault, and in klippen south of Denali fault

MACLAREN TERRANE
(SOUTH OF DENALI FAULT AND NORTH OF BROXSON GULCH THRUST)

East Susitna batholith and schist, quartzite, and amphibolite
South of Denali fault and north of Meteor Peak fault

gg **Gneissose granitic rocks (early Tertiary and Late Cretaceous)**—Chiefly polydeformed quartz diorite and granodiorite, with lesser granite. Relict hypautomorphic-granular texture. Regionally metamorphosed and ductilely deformed at middle amphibolite facies into mylonitic gneiss. Grade into migmatite, migmatitic schist, and schist and amphibolite. Local retrograde, lower greenschist-facies metamorphism

sa **Schist and amphibolite (Late Cretaceous or older)**—Hornblende-biotite-quartz-plagioclase schist and hornblende-plagioclase-quartz amphibolite. Derived from gabbro, quartz gabbro, diorite, quartz diorite, and pelitic sedimentary rocks. Relict hypautomorphic-granular texture in metaigneous rocks. Ductilely deformed and regionally metamorphosed at middle amphibolite facies into mylonitic schist and gneiss. Local retrogressive metamorphism to greenschist facies. Relatively older and more highly metamorphosed equivalent of gneissose granitic rocks (gg) of East Susitna batholith

mig **Migmatite (Cretaceous?)**—Highly contorted schist and amphibolite with abundant, diffuse, thin veins and sills of granodiorite and granite. Gradational unit between gneissose granitic rocks (gg), with fragments of nearly completely assimilated schist and amphibolite (sa), and migmatitic schist (mgsh) units. Contorted schistosity. Contains abundant, small to large granitic dikes

mgsh **Migmatitic schist (Cretaceous?)**—Chiefly schist and amphibolite with sparse to moderately abundant veins of granitic rocks. Attitude of schistosity generally constant over large areas. Gradational unit between schist and amphibolite (sa) and migmatite (mig) units. Contains fewer sills and veins of granitic rocks than migmatite (mig)

sq **Schist, quartzite, and amphibolite (Triassic?)**—Chiefly calc-silicate schist, para-amphibolite, and quartzite. Ductilely deformed and regionally metamorphosed at amphibolite facies into mylonitic schist. Intruded by gneissose granitic rocks (gg)

Maclaren Glacier metamorphic belt
(South of Meteor Peak fault)

mmb **Schist and amphibolite, phyllite, and argillite and metagraywacke (Late Jurassic or older)**—Mainly faulted sequence. Metamorphic grade systematically increases from lower greenschist facies in south to middle amphibolite facies to north. Ductilely deformed into protomylonite and phyllonite in argillite and metagraywacke part of unit, phyllonite in phyllite part of unit, and mylonitic schist in schist and amphibolite part of unit. Found as fault-bounded unit south of Meteor Peak fault and north of Broxson Gulch thrust. Argillite and metagraywacke part of unit mainly derived from volcanic graywacke and siltstone, and minor andesite and basalt, with lesser calcareous and quartz siltstone

CLEARWATER TERRANE
(WITHIN SPLAYS OF BROXSON GULCH THRUST)

csv **Schistose metasedimentary and metavolcanic rocks (Late Triassic)**—Chlorite schist, muscovite schist, and marble. Lesser schistose metarhyolite and metarhyodacite flows, and greenstone derived from pillow basalt. Weakly deformed and metamorphosed at greenschist facies. Intensely deformed at faults between units in some areas

WRANGELLIA TERRANE
(SOUTH OF DENALI FAULT AND BROXSON GULCH THRUST)

JTRm **McCarthy Formation (Early Jurassic and Late Triassic)**—Thin- to medium-bedded calcareous argillite and impure limestone with abundant Monotis. Found in branches of Broxson Gulch thrust

ga **Gabbro, diabase, and metagabbro (Late Triassic?)**—Small, irregular bodies, dikes, and sills of medium- to coarse-grained gabbro and fine- to medium-grained diabase, and locally schistose metagabbro that are found throughout Wrangellia terrane. Gabbro and diabase range from hypautomorphic-granular or ophitic aggregates of clinopyroxene, plagioclase and lesser biotite, to regionally metamorphosed metagabbro composed of schistose aggregates of hornblende or actinolite, chlorite, biotite, epidote, and albite. In some areas, may be late

Paleozoic in age and part of igneous suite in Slana Spur Formation and Tetelna Volcanics

cu **Cumulate mafic and ultramafic rocks (Late Triassic?)**—Moderate- to large-size sills of olivine, olivine-clinopyroxene, and clinopyroxene-plagioclase cumulate. Partly to mostly serpentinized. Locally intensely deformed into serpentinite, actinolite-chlorite schist, or talc schist. Found as large sills in Tangle subterrane, and as fault-bounded lenses in Slana River subterrane

Slana River subterrane
(South of Denali fault and Broxson Gulch thrust and north of Eureka Creek fault)

KJs **Marine metasedimentary rocks (Early Cretaceous and Late Jurassic)**—Interlayered gray argillite, siltstone, graywacke, pebble conglomerate, and andesite. Abundant graded and rhythmic bedding, sole marks, and slump folds in some areas. Interpreted as deep-marine turbidite deposits. Locally isoclinally folded. Weakly metamorphosed to lower greenschist facies

TRl **Limestone (Late Triassic)**—Fine-grained gray limestone to medium-grained gray or white marble. Lenses and nodules of gray and black chert and irregular patchworks of disseminated fine-grained quartz. Thick bedded to massive. Weakly schistose. Pervasively recrystallized. Locally faulted and sheared. Locally faulted into subjacent Nikolai Greenstone. Locally metasomatized to skarn near granitic plutons

TRn **Nikolai Greenstone (Late Triassic)**—Subaerial, amygdaloidal basalt flows separated by thin beds of nonmarine volcaniclastic rocks, chert, and argillite in some areas. Predominantly intermixed aa and pahoehoe flows. Individual flows as thick as several meters. Usually ophitic or hypautomorphic-granular with clinopyroxene, plagioclase, and magnetite. Generally regionally metamorphosed and locally schistose with locally abundant metamorphic actinolite, epidote, chlorite, albite, and sericite. Quartz veins and altered zones areas with Cu-sulfide minerals in some areas

Pe **Eagle Creek Formation (Early Permian)**—Argillite and limestone. Argillite is dark gray and thin bedded and local calcareous siltstone and thin limestone. Limestone is thin bedded to massive and light to dark gray, with thin argillite interbeds. Chert nodules and thin layers of chert, volcanic graywacke, and clastic limestone in some areas. Local grading and crossbedding. Weakly metamorphosed to lower greenschist facies. Locally intensely metamorphosed in some areas near Denali fault

Pi **Shallow-level intrusive stocks, dikes, sills, and small plutons (Early Permian)**—Small- to moderate-size intrusive stocks, dikes, and sills. Mainly dacite with lesser andesite, rhyodacite, and diabase, generally fine grained. Local small plutons of granodiorite and granite. Porphyritic with relict plagioclase phenocrysts in some areas. Weakly schistose in some areas. Weakly metamorphosed to lower greenschist facies. Local intense hydrothermal alteration with replacement of igneous minerals by sericite, chlorite, epidote, actinolite, albite, potassium feldspar, and clay. Local iron staining and disseminated sulfide minerals

Pg **Granitic plutons in Wrangellia terrane (Pennsylvanian)**—Chiefly medium- to coarse-grained hornblende-biotite granodiorite and biotite granite with lesser diorite and quartz diorite. Found in moderate-size and large plutons. Weakly deformed to nonschistose

PPs **Slana Spur Formation (Early Permian to Middle Pennsylvanian)**—Thick sequence of marine calcareous (upper part) and noncalcareous (lower part) volcaniclastic rocks, and lesser volcanic sandstone, conglomerate, tuff, volcanic breccia and flows, and limestone. Fine to coarse grained. Volcanic rocks generally dacite and lesser andesite, rhyodacite, and basalt. Medium to thick bedded. Local abundant graded and crossbedded. Weakly schistose to massive. Pervasively metamorphosed to lower greenschist facies. Local abundant iron staining. Disseminated and massive sulfide minerals

Pt **Tetelna Volcanics (Pennsylvanian)**—Chiefly dark-gray-green andesite and dacite flows, with sparse basalt flows and local volcanic breccia, volcanic graywacke, conglomerate, and tuff. Fine to coarse grained. Thin to thick bedded. Weakly schistose to massive. Pervasively metamorphosed to lower greenschist facies. Local abundant iron staining. Disseminated sulfide minerals

Tangle subterrane
(South of Eureka Creek fault)

TRl **Limestone (Late Triassic)**—Fine-grained gray limestone to medium-grained gray or white marble. Thick bedded to massive. Weakly schistose. Pervasively recrystallized. Found in fault-bounded lenses adjacent to Nikolai Greenstone. Locally faulted and sheared. Locally metasomatized to skarn near granitic plutons

Nikolai Greenstone (Late Triassic)—Divided into:

TRnf **Subaerial basalt flows member** —Subaerial, amydgaloidal basalt flows separated locally by thin beds of nonmarine volcaniclastic rocks and local thin beds of shale, chert, and siltstone. Predominantly intermixed aa and pahoehoe flows. Individual flows as much as few meters thick. Common ophitic texture or hypautomorphic-granular texture with clinopyroxene, plagioclase, and magnetite. Generally regionally metamorphosed and locally schistose with abundant metamorphic actinolite, epidote, chlorite, albite, and sericite. Lithologically similar to Nikolai Greenstone in Slana River subterrane. Local quartz veins and altered areas with Cu-sulfide minerals

TRnp **Pillow basalt flows member** —Massive pillow basalt flows, and minor basaltic breccia and tuff, and argillite. Basalt lithologically similar to subaerial basalt flows of Nikolai Greenstone. Weakly schistose to massive. Generally regionally metamorphosed with abundant metamorphic actinolite, epidote, chlorite, albite, and sericite. Local quartz veins and altered areas including Cu-sulfide minerals

Pzt **Aquagene tuff, argillite, limestone, chert, andesite tuff, and greenstone (late Paleozoic)**—Interlayered basaltic aquagene tuff, gray siliceous argillite, calcite limestone, and marble, red and black chert, and gray-green tuff and basalt. Medium to thick bedded. Weakly schistose to massive. Pervasively metamorphosed to lower greenschist facies

GULKANA RIVER TERRANE
(SOUTH OF PAXSON LAKE FAULT)

mha **Metamorphosed hornblende andesite (late Paleozoic?)**—Chiefly unfossiliferous weakly metamorphosed hornblende andesite and lesser clinopyroxene basalt. Massive to weakly schistose. Correlative with Haley Creek metamorphic assemblage of Plafker and others (1989) in northern Valdez quadrangle to southeast that contains lithologically similar late Paleozoic metamorphosed andesite and basalt flows

CORRELATION OF MAP UNITS

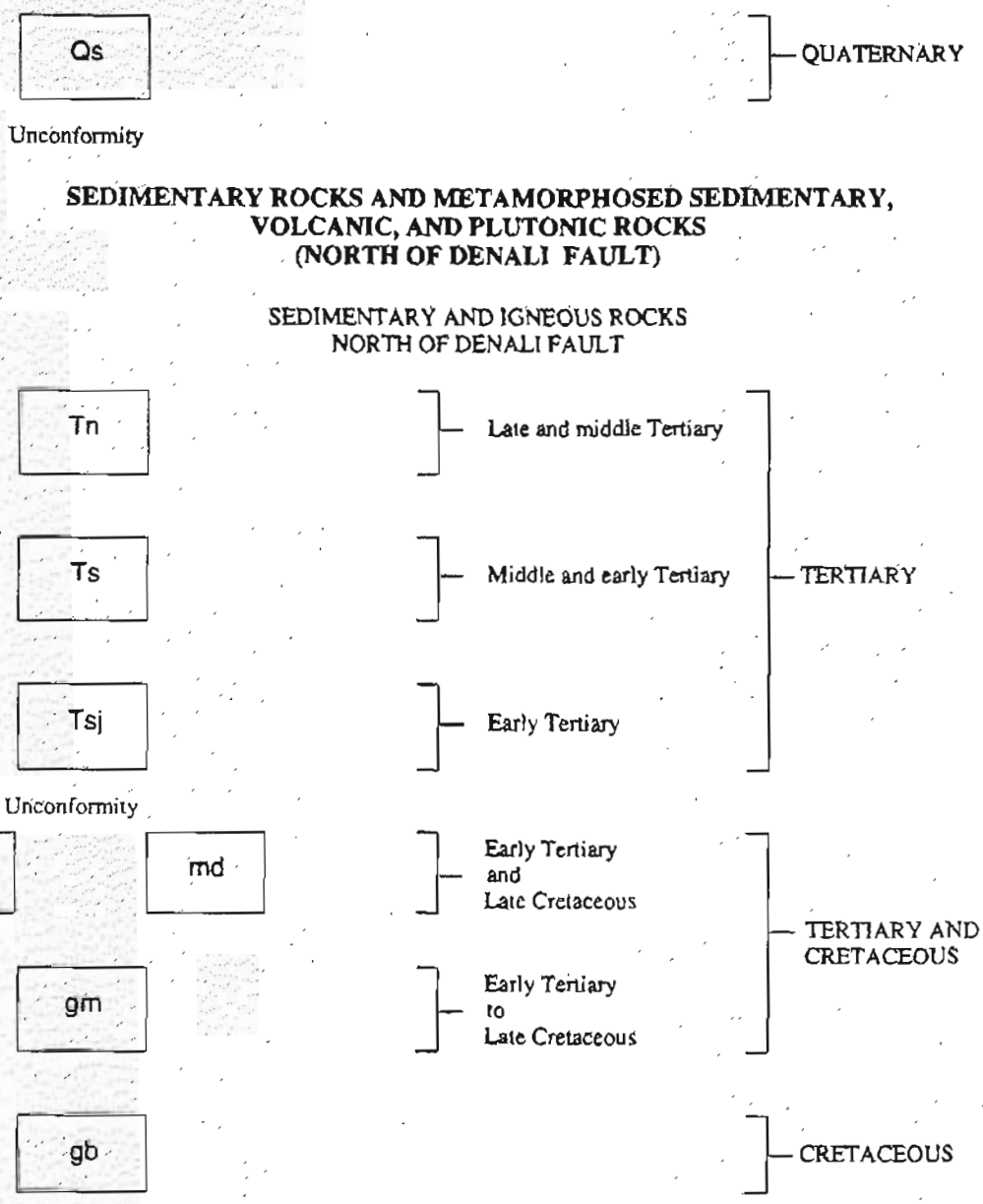

YUKON-TANANA TERRANE

Lake George subterrane
(North of Tanana River fault)

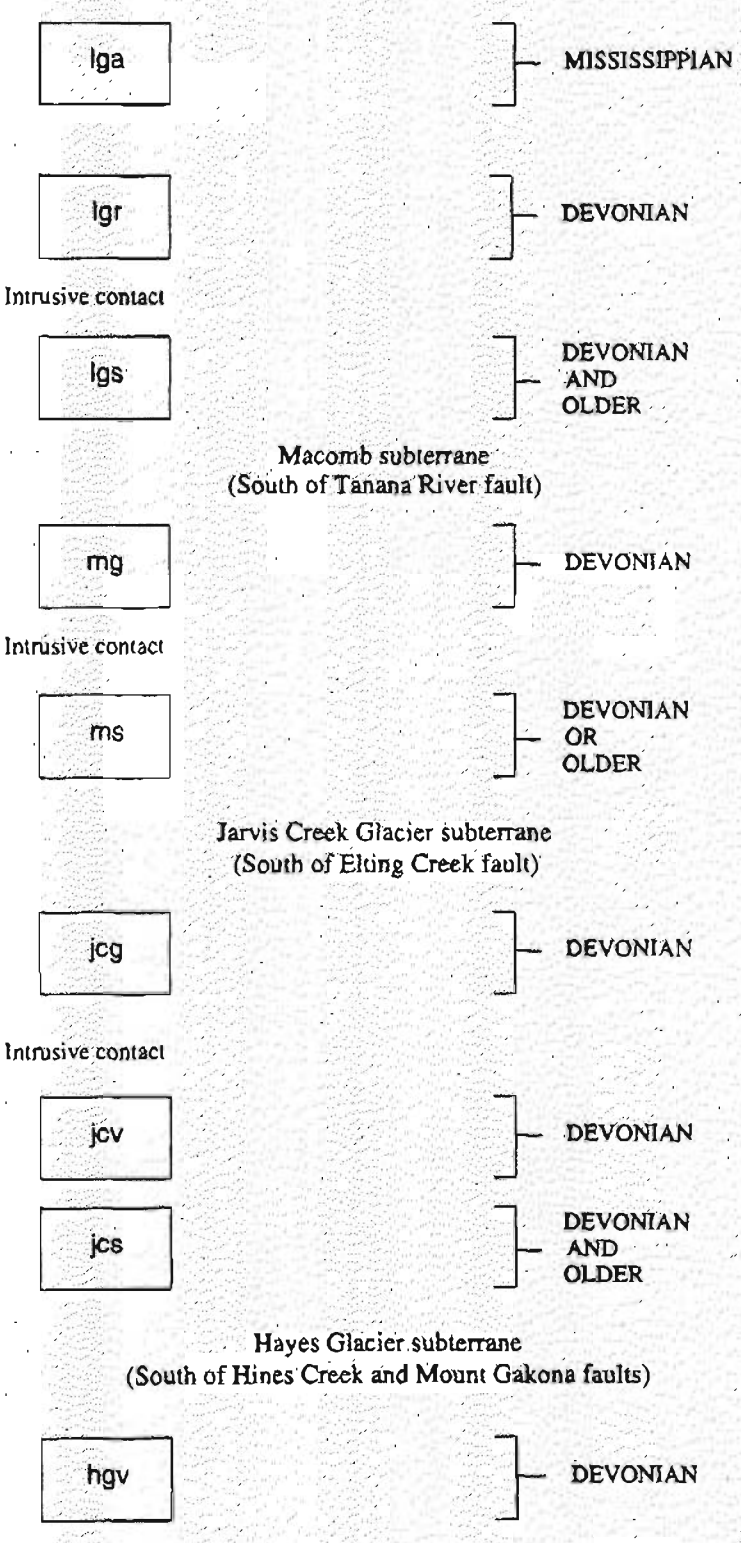

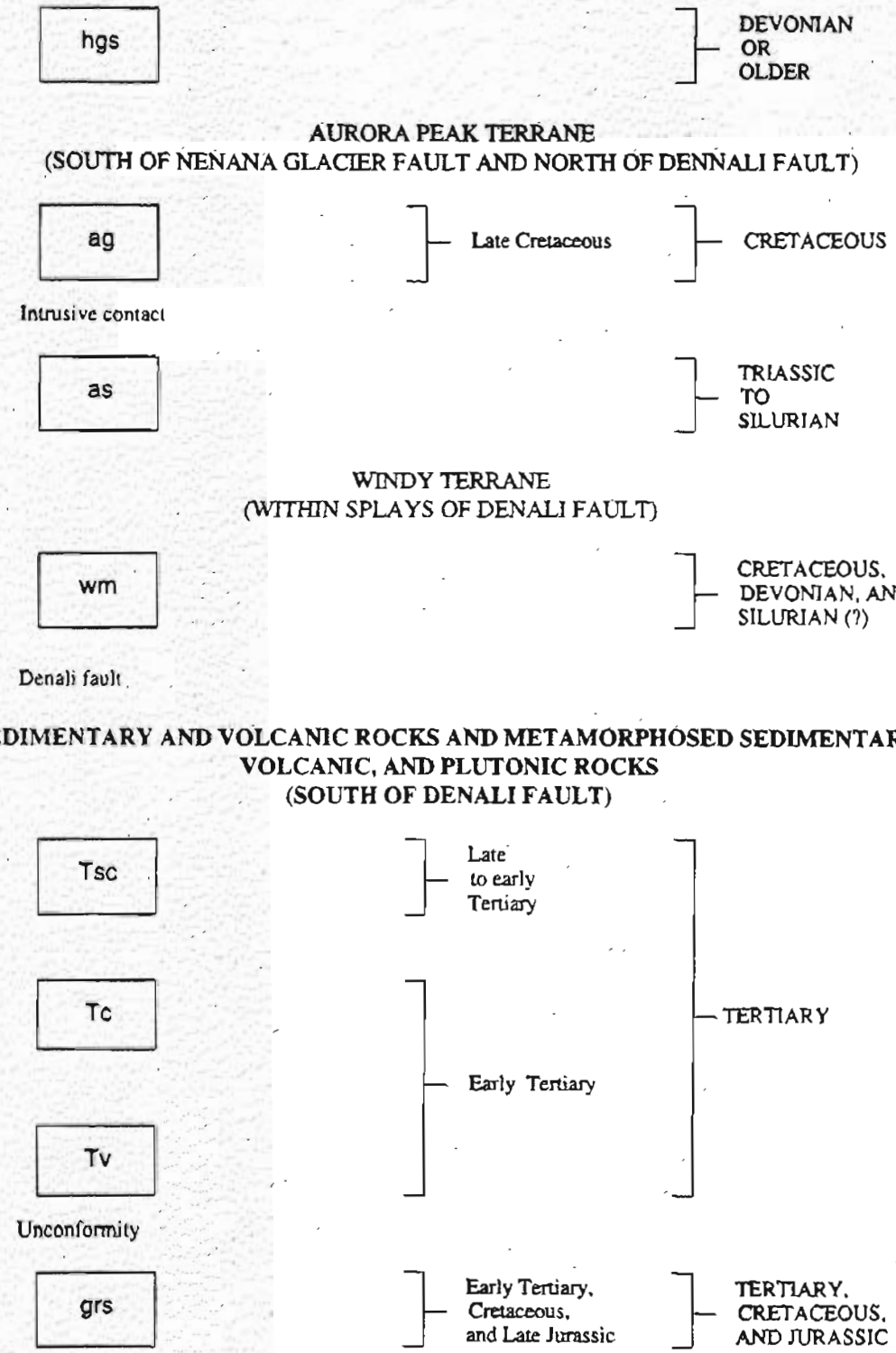
hgs
DEVONIAN OR OLDER
AURORA PEAK TERRANE
(SOUTH OF NENANA GLACIER FAULT AND NORTH OF DENNALI FAULT)
ag
Late Cretaceous
CRETACEOUS
Intrusive contact
as
TRIASSIC TO SILURIAN
WINDY TERRANE
(WITHIN SPLAYS OF DENALI FAULT)
wm
CRETACEOUS, DEVONIAN, AND SILURIAN (?)
Denali fault
SEDIMENTARY AND VOLCANIC ROCKS AND METAMORPHOSED SEDIMENTARY, VOLCANIC, AND PLUTONIC ROCKS
(SOUTH OF DENALI FAULT)
Tsc
Late to early Tertiary
Tc
Early Tertiary
TERTIARY
Tv
Unconformity
grs
Early Tertiary, Cretaceous, and Late Jurassic
TERTIARY, CRETACEOUS, AND JURASSIC

TERRANE OF ULTRAMAFIC AND ASSOCIATED ROCKS

um		MESOZOIC(?)

Splay of Denali fault

MACLAREN TERRANE
(SOUTH OF DENALI FAULT AND NORTH OF BROXSON GULCH THRUST)

East Susitna batholith and schist, quartzite, and amphibolite
South of Denali fault and North of Meteor Peak fault

gg	Early Tertiary and Late Cretaceous	TERTIARY AND CRETACEOUS
sa	Late Cretaceous or older	CRETACEOUS OR OLDER
mig		CRETACEOUS(?)
mgsh		

Intrusive contact

sq		TRIASSIC(?)

Maclaren Glacier metamorphic belt
(South of Meteor Peak fault)

mmb	Late Jurassic or older	JURASSIC OR OLDER

CLEARWATER TERRANE
(WITHIN SPLAYS OF BROXSON GULCH THRUST)

cvs	Late Triassic	TRIASSIC

WRANGELLIA TERRANE
(SOUTH OF DENALI FAULT AND BROXSON GULCH TRUST)

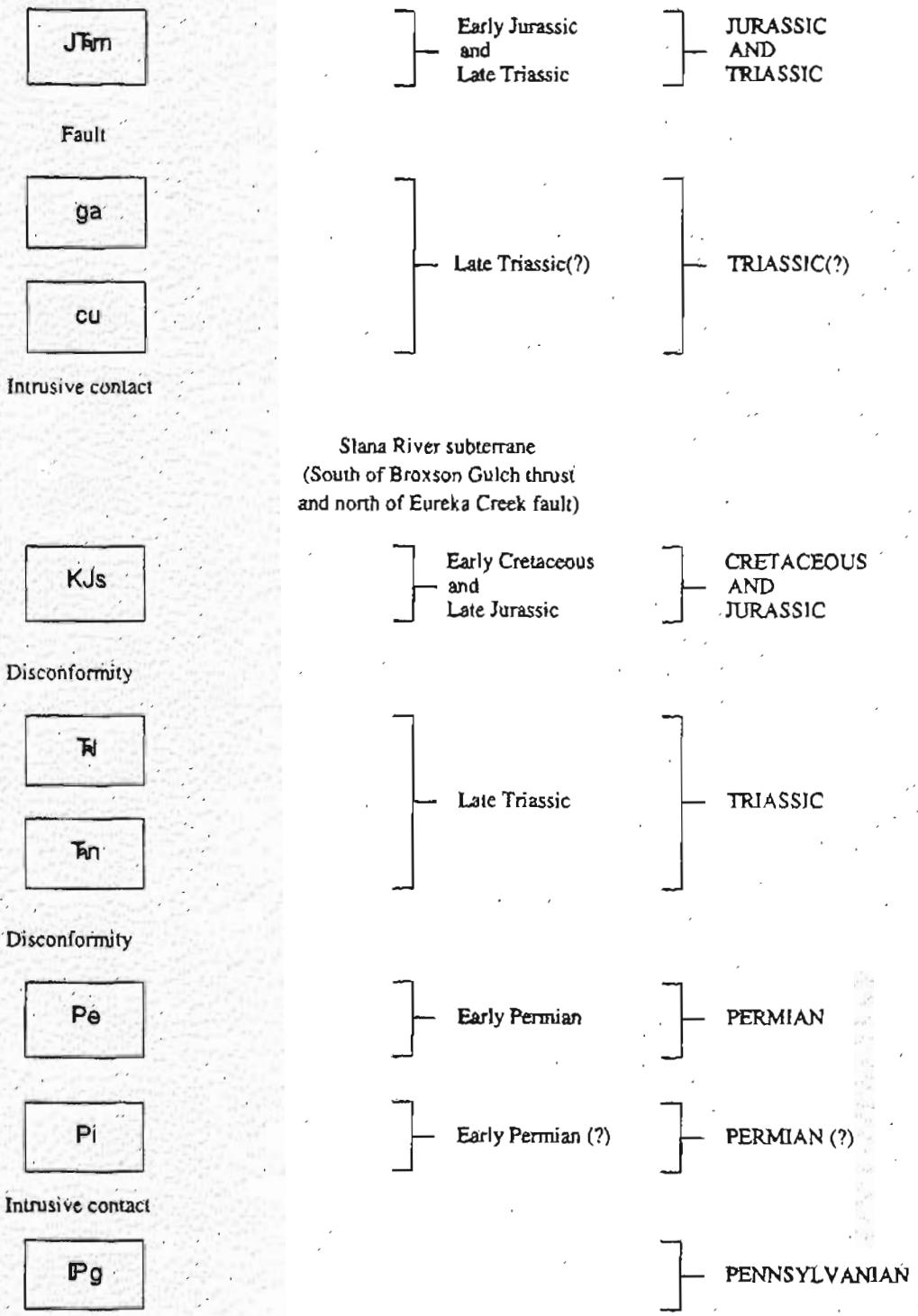

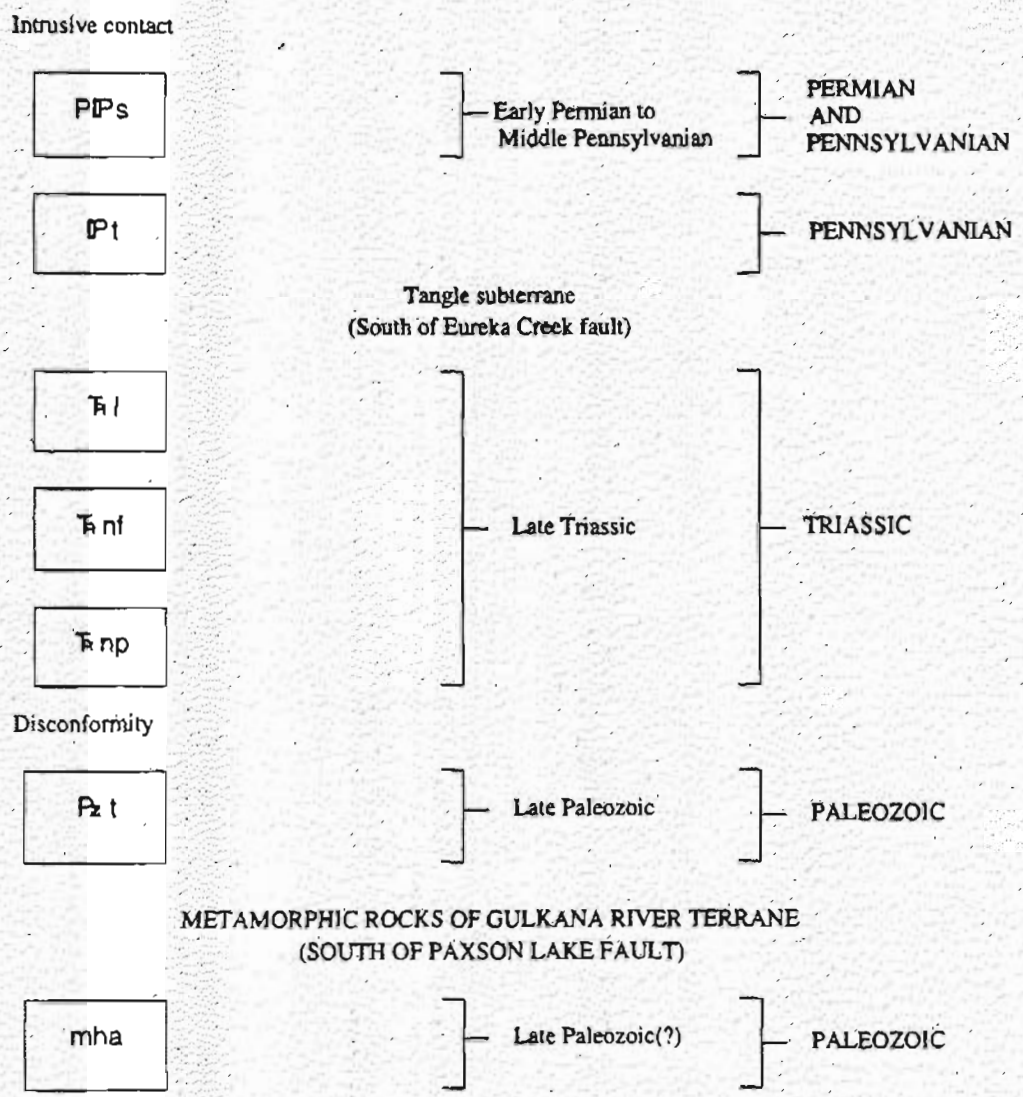
Intrusive contact
PIPs
Early Permian to Middle Pennsylvanian
PERMIAN AND PENNSYLVANIAN
IPt
PENNSYLVANIAN
Tangle subterrane
(South of Eureka Creek fault)
Trl
Trnf
Trnp
Late Triassic
TRIASSIC
Disconformity
Pz t
Late Paleozoic
PALEOZOIC
METAMORPHIC ROCKS OF GULKANA RIVER TERRANE
(SOUTH OF PAXSON LAKE FAULT)
mha
Late Paleozoic(?)
PALEOZOIC